Genetic and immunological characterization of a hyper-IgE Syndrome pedigree

Master Thesis

Master in Biotechnology for the Health Sciences

Diana Raquel Carneiro Pombal

Work done under the supervision of

Professor Dr. Adrian Liston

and co-supervision of

Professor Dr. Patrícia Poeta

University of Trás-os-Montes e Alto Douro

Vila Real, 2013

Genetic and immunological characterization of a hyper-IgE Syndrome pedigree

Master Thesis

Master in Biotechnology for the Health Sciences

Diana Raquel Carneiro Pombal

Work done under the supervision of

Professor Dr. Adrian Liston

and co-supervision of

Professor Dr. Patrícia Poeta

University of Trás-os-Montes e Alto Douro

Vila Real, 2013

Orientador:

Professor Doutor Adrian Liston

Co-orientadora:

Professora Doutora Patrícia Poeta

Directora do 2° Ciclo:

Professora Doutora Paula Lopes

Aluna:

Diana Raquel Carneiro Pombal

Júri de Apreciação

Presidente:_____

1° Vogal:_____

2° Vogal:_____

Classificação:_____

Data:_____, _____ de _____ de _____

Este trabalho foi realizado no Departamento de Medicina da Katholieke Universiteit Leuven sob a supervisão do Professor Doutor Adrian Liston.

Acknowledgements

As I finish my masters, I look back and see people to whom I can't but thank for the opportunities, the trust, the encouragements, the teachings, the care and friendship. Without them it would have been much harder to get here.

First of all, I thank my supervisor Prof. Adrian Liston for the opportunity of studying in this lab and for the exciting projects, the incentive, the trust and the supportive criticism that helped grow and want to do better. Thank you for the indispensable help in writing this thesis. I also want to congratulate him for putting together so many incredible people that make this lab one-of-a-kind.

Thank you to my co-supervisor, Prof. Patrícia Poeta for accepting co-supervising me knowing this thesis would be done outside Portugal. I thank her for the advice, patience and trust.

I want to thank the presidency of the school and the coordination of the master's degree for accepting this project.

To Kim, I thank for being my mentor, whose huge help was vital. I want to also thank her for the incentives, teachings, availability, criticism and, of course, for the friendship, advice, care and enthusiasm, which was and continues to be so welcome.

Thank you, to all my friends and colleagues from the lab; to Susan and James for all the help, teaching, trust, patience and friendship; to Dina, who was the person with whom I interacted most when I arrived in the lab and who taught much. Thank you Dean for the sarcasm and jokes, you're a genius. To Lien, I have to thank for all the help with the clinical part of my thesis and the fun moments working together. To Lei, Jay and Jossy, thank you for the friendship, companionship, for the fun moments, the chats and advice. I thank Stephanie, Benedict, Anh and Yulia for being the sweetest persons. To Simon, Wim and Susann thank you for simply being brilliant. Thank you all.

To my every-moment friends, Manu, Carlota and Lis, thank you for the love, sincerity, care, lectures and for all the support that helped me grow and become better. Thank you to Magda and Joana Guedes who were with me in some tough moments and are proof that there's always a bright side in life.

To all my family, thank you for the unconditional love, for the principles you taught me and still do, for the care and reprehensions, for teaching me to stand so I could walk. I specially thank my mother, for all the strength, for always pushing me forward, for the teachings and advices, for simply being the remarkable person she is.

Abstract

Understanding the immune system and how it is influenced by the genome are key steps for unraveling the genetic basis of immunological regulation and dysregulation. Advances in genetic tools and sequencing strategies potentially allow us to identify novel disease-causing mutations in poorly understood diseases such as hyper-IgE syndrome (HIES). HIES is a primary immune deficiency characterized by eczema, recurrent skin and lung infection, and greatly increased serum levels of IgE. HIES has been linked to a Mendelian inheritance of mutations in *STAT3, DOCK8* and *TYK2,* however, most cases do not have a known genetic cause. In this study we worked on a family which manifested two cases of HIES in children of consanguineous parents. The patients of this study were diagnosed with HIES, yet no mutation in *STAT3, DOCK8* or*TYK2* were found. Resorting to whole-exome sequencing we found a rare coding SNP in *CARD11,* which was considered the best candidate to explain the patient's phenotype due to the similarities to the Card11-deficient mouse phenotype (atopic dermatitis, increased serum levels of IgE and Th2-driven immune response). Based on this we hypothesized that this SNP was causing HIES in the patients, however our results rule out *CARD11* as the causable gene for the clinical phenotype. The immune phenotyping of one of the patient revealed a decrease in Th2 cells, T_{regs} and naïve $CD4^+$ T cells, and an increase in memory $CD4^+$ and $CD8^+$ T cells. Together, these results suggest a novel category of HIES, in genetic and immunologic basis. Additional research to identify the disease causation in this family may contribute for the better understanding of IgE production and IgE-mediated diseases.

Resumo

Compreender o sistema imunológico e como é influenciado pelo genoma são processos fundamentais para desvendar a base genética da regulação e desregulação imunológica. Os avanços das ferramentas genéticas e estratégias de sequenciação potenciam a identificação de mutações causadoras de doenças mal compreendidas como a síndrome de hiper-IgE (HIES). HIES é uma imunodeficiência primária cujas características incluem eczema, infecções pulmonares recorrentes e níveis séricos de IgE extremamente elevados. HIES tem sido associada à herança mendeliana de mutações em *STAT3*, *DOCK8* e *TYK2*, no entanto, a maior parte dos casos não tem causa genética conhecida. Neste estudo, trabalhamos uma família com dois casos de HIES. Os pacientes deste estudo, filhos de pais consanguíneos, foram diagnosticados com HIES, no entanto nenhuma mutação foi encontrada em *STAT3*, *DOCK8* ou *TYK2*. Recorrendo a "whole-exome sequencing" encontrou-se um SNP codificante raro em *CARD11*. Este SNP foi considerado o melhor candidato para explicar o fenótipo do paciente, devido às semelhanças com o fenótipo murino de deficiência em *Card11* (dermatite atópica, aumento dos níveis séricos de IgE e resposta imune mediada por células Th2). Com base nisto, a hipótese de que este SNP era a causa de HIES nos doentes foi formulada. Contudo, os nossos resultados excluem *CARD11* de ser o gene causador do fenótipo clínico. A elaboração do perfil imunológico de um dos paciente revelou uma diminuição de células Th2, T_{regs} e células T $CD4^+$ naïve, e um aumento nas células $CD4^+$ em $CD8^+$ de memória. Em suma, estes resultados sugerem que a HIES apresentada pelos pacientes pertence a uma nova categoria, quer de foro genético, quer de foro imunológico. Pesquisa adicional é necessária para identificar a causa da doença nesta família e pode contribuir para uma melhor compreensão da produção de IgE e de doenças mediadas por IgE.

Abbreviations

ABC-DLBCL – activated B cell-like DLBCL
ADA – Adenosine deaminase
AD-HIES – Autosomal dominant HIES
AID – Activation-induced cytidine deaminase
ALPS – Autoimmune lymphoproliferative syndrome II
APC – Antigen presenting cells
AR-HIES – Autosomal recessive HIES
BCL10 – B cell lymphoma 10
BCL6 – B cell lymphoma 6
BCR – B cells receptor
BIMP3 – BCL10-interacting MAGUK protein 3
BGI – Beijing Genomics Institute
C/EBP – CCAAT/enhancer binding protein
CARD11 – Caspase recruitment domain family, member 11
CARMA1 – CARD-containing MAGUK protein 1
CBL – Casitas B-lineage lymphoma proto-oncogene
CBM – CARD11-BCL10-MALT1 complex
CCL – CC chemokine ligand
CCR – CC chemokine receptor
CD – Cluster of differentiation
cDNA – complementary DNA
CSR – Class switch recombination
CTLA4 – Cytotoxic T-lymphocyte-associated protein 4
DC – Dendritic cell
DLBCL – Diffuse large B cell lymphoma
DMSO – Dimethyl sulfoxide
DNA – Deoxyribonucleic acid
DOCK8 – Dedicator of cytokinesis 8
dsRNA – Double stranded RNA
E2A – TCF3; transcription factor 3
EDTA – Ethylenediaminetetraacetic acid

ELISA – Enzyme-Linked Immunosorbent Assay

FACS – Fluorescence-activated cell sorting

FBS – Fetal bovine serum

FLG – Filaggrin

FOXP3 – Forkhead box P3

GAPDH – Glyceraldehyde 3-phosphate dehydrogenase

GATA3 – GATA binding protein 3

GC – Germinal center

G-CSF – Granulocyte-colony stimulating factor

gDNA – genomic DNA

GFP – Green fluorescent proteins

GWAS – Genome wide association studies

HEL – Hen egg lysozyme

HIES – Hyper-IgE sindrome

HLA-DRB1 – Major histocompatibility complex, class II, DR beta 1

HPRT – Hypoxanthine-guanine phosphoribosyltransferase

ICAM – Intercellular adhesion molecule

ID2 – Inhibitor of DNA binding 2

IFN – Interferon

IgA – Immunoglobulin A

IgD – Immunoglobulin D

IgE – Immunoglobulin E

IgG – Immunoglobulin G

IgM – Immunoglobulin M

IKK – IκB kinase

IL- Interleukine

IPEX – Immunodysregulation polyendocrinopathy enteropathy X-linked syndrome

iT_{regs} – Inducible T_{regs}

IVIG – Intravenous immunoglobulin

KO – knock out

LB – Lysogenic Broth

LFA-1 - Lymphocyte function-associated antigen 1

LPS – Lipopolysaccharides

LSM – Lymphocyte separation media

MAGUK – Membrane-associated guanylate kinase

MALT1 – Mucosa associated lymphoid tissue lymphoma translocation gene 1

MHC – Major histocompatibility complex

mIgE – membrane-bound IgE

mRNA – message RNA

NF-κB – Nuclear factor of kappa light polypeptide gene enhancer in

NK cells – Natural killer cells

NKT – Natural killer T cells

NMS – Normal mouse serum

NOD – nucleotide-binding oligomerization domain receptors

NRL – NOD-like receptors

PAX5 – Paired box 5

PBMC – Peripheral blood mononuclear cell

PBS – Phosphate buffered saline

PCR – Polymerase chain reaction

PMA – Phorbol myristate acetate

qPCR – Quantitative PCR

RIPK2 – Receptor-interacting serine-threonine kinase 2

RNA – Ribonucleic acid

ROR-γt – Retinoic acid-related orphan receptor γt

Rpm – rotation per minute

RPMI – Roswell Park Memorial Institute medium

RT – Room temperature

RT-PCR – Real time PCR

RTE – Recent thymic emigrant

SCID – Severe combined immunodeficiency

SD – Standard deviation

SLP-76 – SH2 domain-containing leukocyte protein of 76kD

SNP – Single nucleotide polymorphism

SOCS – Suppressor of cytokine signaling

STAT3 – Signal transducer and activator of transcription 3

STAT6 – Signal transducer and activator of transcription 6

TBE – Tris-Borate-EDTA buffer

TCM – Central memory T cells

TCR – T cell receptor

TEM – Effector memory T cells

TEMRA – TEM $CD45R^{+}$

TGF-β – Transforming growth factor beta

Th cells – helper T cells

Tfh cells – follicular helper T cells

TLRs – Toll-like receptors

TNFα – Tumor necrosis factor alfa

T_{regs} – Regulatory T cells

Unm – unmodulated

TYK2 – Tyrosine kinase 2

WES – Whole exome sequencing

WT – wild type

ZAP-70 – Zeta-chain (TCR) associated protein kinase 70kDa

Contents

Figure Index

Table Index

1 Introduction

Exploring the influence that the genetic background exerts over the immune system is fundamental for the understanding of its regulation and dysregulation. Hyper-IgE syndrome (HIES) is a rare primary immune deficiency, and although the genetic basis for many cases of familiar HIES has been explained with the identification of Mendelian mutations in *STAT3, DOCK8* and *TYK2,* most HIES cases remain unexplained, with unknown genetic origin. Advances in genetic tools, notably the blueprint of the human genome created through the human genome project and the advent of next-generation sequencing increases our ability to identify novel mutations that make up the "genetic dark matter" of unexplained HIES. Using whole exome sequencing technology is possible to investigate candidate genes associated to a particular disease by studying the likely affected pathways, culminating in the identification of therapeutic molecular targets.

1.1 Immune system overview

1.1.1 Immune system differentiation

The immune system is responsible for the protection of the body from infectious organisms, a function which necessitates the distinction between "self" and "non-self". Immune reactions are mediated by immune cells, or leukocytes, that develop from hematopoietic precursor cells in the bone marrow [1]. The first stage in hematopoietic differentiation commits the self-renewing hematopoietic stem cells into one of the two major branches – the myeloid precursor or lymphoid precursor. The myeloid precursor gives rise to both non-leukocytes (red blood cells and platelets) and a large range of myeloid leukocytes, including granulocytes (basophils, eosinophils and neutrophils), mast cells, monocytes and most macrophages and dendritic cells [1]. In turn, the lymphoid precursor is the progenitor cell for NK cells, T cells, B cells and also dendritic cells and macrophages [1]. All leukocytes differentiate in the bone marrow, with the exception of T cells, which require the migration of the lymphocyte precursor to the thymus [1].

1.1.2 Innate immunity

Immune mechanisms may be divided into two main lines of action, innate immunity and adaptive immunity, which have fundamentally different mechanisms for

identifying non-self and yet act in complementary manners. The first line of defense pathogens encounter is barrier immunity which involves the action of mechanical, chemical and physiological barriers. Pathogens that evade barrier immunity encounter the innate immune system, which acts non-specifically against pathogens through the activation of the cells of the innate immune system [2]. Among the later are phagocytes, basophils, eosinophils, mast cells, dendritic cells and NK cells [2]. The innate immune system acts through a selection of pattern recognition receptors which may be expressed on the cellular surface and intracellularly or secreted into the blood and tissue fluids [2]. Among the intracellular receptors there are the protein kinase PKR and the OAS/RNaseL pathway, which activate when bound to viral dsRNA. The first blocks protein synthesis, both viral and cellular, promotes the expression of antiviral type-I IFN genes and induces the apoptosis of infected cells. The second cleaves both viral and cellular RNAs, which, like PKR, blocks protein synthesis and promotes the apoptosis of infected cells [2].

In addition to PKR and OAS/RNaseL, the family of nucleotide-binding oligomerization domain receptors (NOD) is also involved in intracellular pattern recognition [2]. The pathogen recognition receptors from this family are called NOD-like receptors (NLRs). NLRs can be classified into two subgroups, NLR*C*, which contains a *Card* domain, and NLR*P*, which contain a *Pyrin* domain [3]. NOD1 and NOD2 proteins belong to the NLR*C* group and are an important piece in pathogen recognition, specially the recognition of peptidoglycan moieties and activation of immune responses [3]. Upon recognition, NLR signals the recruitment of cooperating proteins, which lead to the interaction of the CARD domain with CARD-containing kinase RIPK2 and culminates in the activation and translocation of NF-κB to the nucleus, which in turn promote the expression of proinflammatory genes [3].

Another key family of pattern recognition receptors expressed on cells from the innate immune system are the Toll-like receptors (TLRs). These proteins are expressed in the cell membrane and in subcellular organelles and recognize specific pathogen components and induce the expression of costimulatory molecules [2,4,5]. Ten different TLRs have been identified in humans and thirteen in mice; TLR1-9 are conserved between the two species while TLR10 is expressed only in humans [5]. TLR can be grouped in 5 subfamilies, TLR3, TLR4, TLR5, the TLR2 family (TLR1, TLR2, TLR6 and TLR10) and the TLR9 family (TLR7, TLR8 and TLR9) [4]. Each TLR differs from the others in its ligand specificity and expression patterns [2]. For instance, TLR4

recognizes LPS from gram-negative bacteria and mannan in fungus, while TLR2 recognizes peptidoglycan in gram-positive bacteria and TLR9 recognizes bacterial and viral DNA. The activation of the innate immune response, via the recognition of the pathogen molecular patterns, initiates effector mechanisms that can induce an adaptive immune response. This process is primarily driven by the uptake and presentation of antigens by antigen-presenting cells (APCs), and the secretion of proinflammatory cytokines and chemokines, which activate, attract and drive the differentiation of T cells [2,6].

1.1.3 Adaptive immunity

The activation of the adaptive immune response depends on two events, the recognition of a specific antigen and the generation of the immune response against it. The function of the adaptive immune system requires the generation of numerous antigen receptor specificities by somatic mechanisms of gene rearrangements and receptor diversification [6]. Both B cells and T cells undergo a maturation phase where the series of genes that encode the cell's antigen-binding receptor undergoes random rearrangements, generating a large diversity of specific antigen-binding receptors [7]. The assembly of functional immunoglobulin genes depends on genetic recombination and DNA modification mechanisms. It occurs during B cell differentiation, within the bone marrow and germinal centers, and involves the rearrangement of variable-region and promotes the generation of specific antibodies against a wide spectrum of potential antigens [8–10] (Figure **1**) [9,11]. During this process individual heavy-chain variable (V_H), diversity (D) and joining (J_H) gene segments randomly combine with imprecise joints to generate a $V_H(D)J_H$ cassette that encodes for a specific V_H domain [7,9]. A similar process occurs with the light-chain, with the resulting recombined heavy and light chains forming the unique immunoglobulin produced by each B cell. T cells undergo a similar process to generate the T cell receptor (TCR), but using a different gene set.

The production of unique immunoglobulins and TRCs gives rise to an array of semi-random receptors clonally distributed on T and B cells with the potential to recognize almost any antigenic structure that might be associated with infectious pathogens [6]. In contrast to the innate immune system, which relies on the recognition of conserved molecular patterns expressed on pathogens, the adaptive immune system recognizes specific antigens without any requirement of evolutionary conservation. In the case of B cells, antigens can be recognized with no further requirements, but in the

case of T cells, antigen recognition requires the expression of antigens presented by major histocompatibility complex (MHC) molecules [6]. The activation of the adaptive immune response is initiated at the moment of infection and takes over when the innate defenses are not enough to stop the infection [12]. The adaptive immune system is capable of recognizing and eliminating specific pathogens and displays particular characteristics: (1) antigenic specificity; (2) diversity; (3) immunologic memory; and (4) self/non-self recognition [7].

For an effective immune response two types of cells need to be present: lymphocytes (B cells and T cells) and APCs [7]. The TCR expressed by T cells can only recognize foreign peptides when they are bound to molecules from the MHC [7]. This means that antigens must be displayed on the surface of the body's own cells, such as APCs, B cells and infected, damaged, or tumorous cells [12]. Antigen-presenting cells phagocytose and display antigenic peptides bound to MHC molecules to T cells, which become activated after recognizing this complex. MHC has two main classes, MHC class I and MHC class II, which are solely recognized by CD8 T cells and CD4 T cells, respectively. CD4 T cells secrete many cytokines that activate other cells, such as B cells, CD8 T cells and macrophages [7]. CD8 T cells have the main role of screening and eliminating altered cells (tumor cells, virus infected cells) by resorting to their cytotoxic characteristics [7]. CD4 T cells may be divided into effector/helper T cells (including Th1, Th2 and Th17) and regulatory T cells. As mentioned above, phagocytic cells are involved in activating the adaptive immune response, nevertheless the inverse is also true. Various factors produced during the adaptive immune response can enhance the activity of phagocytes [7]

While T cells only recognize antigens when they are presented with MHC molecules, B cells are able to do so on antigens alone [7]. B lymphocytes or B cells are adapted to recognize soluble antigens through their receptor, which is a membrane-bound form of immunoglobulin [7,12]. After recognition, they internalize the antigen, process it and display the peptide fragments together with MHC class II [12]. The peptide:MCH class II complex is recognized by antigen-specific CD4 T cells [12]. As a result of the interaction between the CD4 T cell and B cell, the T cell secretes cytokines that influence B cell differentiation into memory B cells, which gain a longer life span and keep the receptor, or effector B cells (plasma cells), which lose the membrane-bound form of immunoglobulin but produce a secretory form of the protein with the same specificity, known as antibody [7]. The large diversity of immunoglobulin

sequences produced during B cell differentiation is expanded by interaction with activated T cells in the process known as somatic hypermutation. Somatic hypermutation is central to provide a structural substrate for the positive selection of higher affinity mutants to specific antigens [11] in the affinity maturation process [10]. During this stage there is a massive accumulation of point mutations in the region between the immunoglobulin promoter and the intronic immunoglobulin enhancer of the V genes of the heavy and light chain.

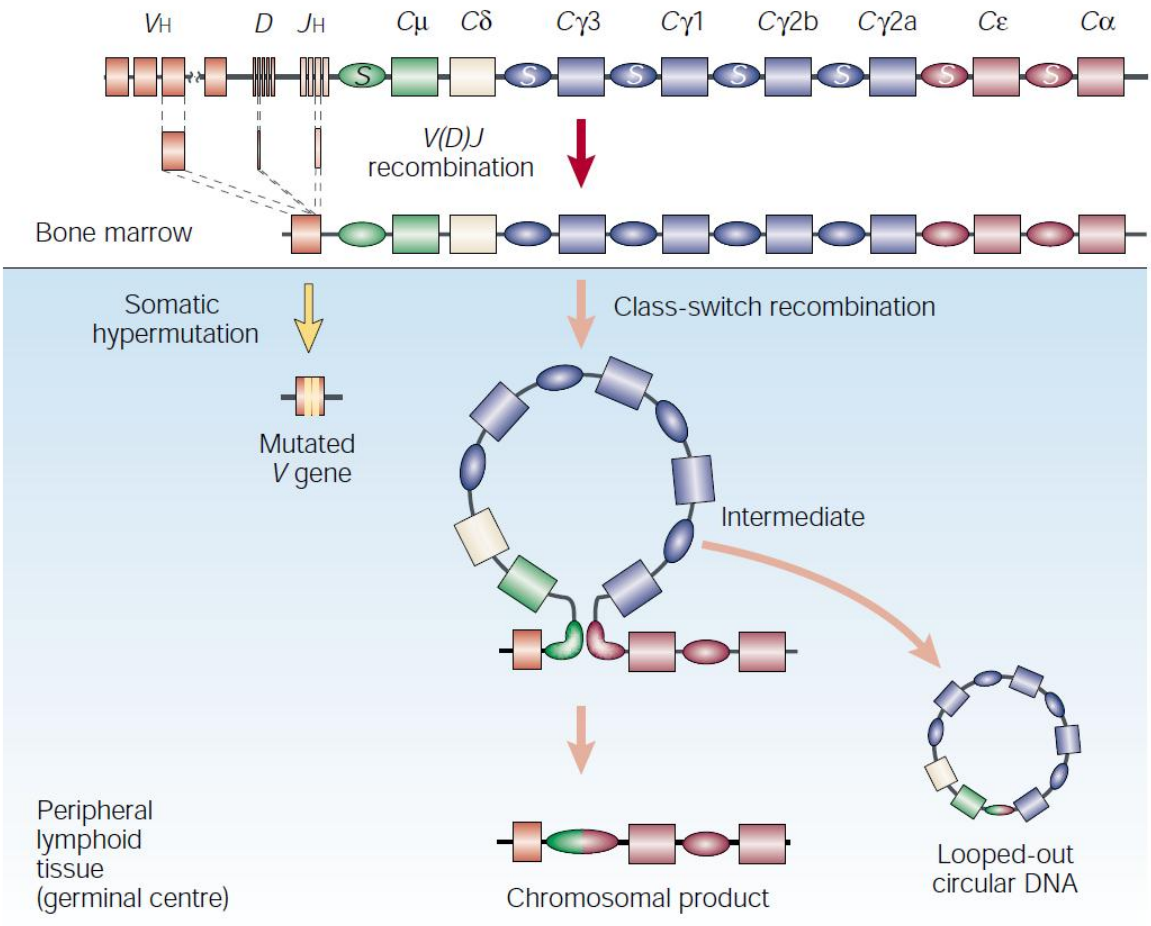

Figure 1 – Representation of the immunoglobulin heavy-chain gene rearrangement [10]. The assembly of V_H, D and J_H gene segments by somatic recombination, the somatic hypermutation of the V gene and Class-switch recombination towards different immunoglobulin isotype contribute for the highly variable pool of functional immunoglobulins.

Initially all B cells express IgM and IgD, but upon appropriate stimuli they are able to switch antibody isotype while maintaining their antigen specificity [9,13]. B cells can potentially produce five types of immunoglobulins: IgM, IgG, IgA, IgD and IgE, although individual B cells will only produce one secretory form at a time.

Overall, immunoglobulins have the ability to recognize antigens and to invoke responses, but each isotype has a different functional property [7]. This variability of functions results from interactions between heavy-chain constant regions and other serum proteins or cell-membrane receptors [7]. This ability to alter the isotype of the antibody is gained during a process called class switch recombination (CSR), which is the last stage for the assembly of functional immunoglobulins. CSR alters irreversibly the C_H cassettes of the immunoglobulin isotypes and gives rise to different heavy chains[9].

1.1.4 Immune dysregulation

The role of the immune system is to defend the organism against pathogens, while preserving tolerance to its own tissues [14]. The mechanisms involved in ensuring self-tolerance include clonal deletion, anergy, ignorance, exhaustion, regulatory T cells (T_{regs}), and cytokine deviation [14]. Despite the critical role of the immune system in protecting the body against infection, in some cases the complex immunological interactions that produce immunological tolerance towards self and innocuous non-self fail in their protective role. When this occurs, the immune system can develop exacerbated reactions to innocuous antigens or direct immune reactions against self-antigens, leading to allergies and autoimmune diseases, respectively. These diseases of immune dysregulation can be divided into two main groups: primary immune dysregulations, which are congenital and are the result of mutations in immune-related genes, and secondary immune dysregulations, which are acquired and are caused by other diseases, environmental factors or medication [12]. The focus of this work will be on primary immune dysregulation that include elevated immunoglobulin E (IgE) production, most importantly HIES.

1.2 Immunoglobulin E

IgE was the last immunoglobulin to be identified. Its identification was the product of Kimishige and Teruko Ishizaka's work in 1966 while studying the possibility of a unique immunoglobulin, other than the ones known at the time, being associated with the human reaginic antibody [15]. IgE is composed of two identical heavy chains and two identical light chains, covalently bound. As with other immunological isotypes,

both chains are comprised by a variable region, which dictates antigen-specificity and a constant region, which dictates many of the functional aspects [16–18]. IgE can be found in two forms: secretory IgE and membrane-bound IgE (mIgE)[8]. The difference between the two forms is the addition of an extracellular membrane proximal domain, a transmembrane sequence and a cytoplasmatic tail on the last constant domain of the heavy chain of mIgE [19–22]. mIgE is used for the activation of isotype-switched B cells, with secretory IgE being the functional mediator.

IgE is produced by B cells and plasma cells in the mucosal-associated lymphoid tissue, after which is rapidly removed from circulation and bound by IgE recepors [8,23]. IgE has two types of receptors, a low-affinity receptor (FcεRII or CD23) and a high-affinity receptor (FcεRI). FcεRII is expressed by numerous immune cells. In B cells, when IgE binds to this receptor, it facilitates the antigen uptake and promotes presentation to T cells [8] , increasing the secondary immune response[9]. Cross-linking of this receptor and the antigen-serum IgE complex on B cells' membrane, results in suppression of IgE synthesis. However, sCD23 (the soluble form of FcεRII) has been shown to enhance IgE production. FCεRI and FCεRII bound to APCs and B cell's membrane, respectively, also contribute to antigen presentation to T cells. Antigen-IgE-FCεRI/FCεRII complexes are transported from the cell surface, processed and presented together with MHCII antigens [8].

These interactions mediate a homeostatic mechanism in the regulation of IgE production [7,8,13].

The main functional mediator of IgE is through the high-affinity receptor (FCεRI). FCεRI is highly expressed by mast cells and basophils, which are the main mediators of IgE function, although it is also expressed at a lower level by neutrophils, monocytes, macrophages, dendritic cells, Langerhans cells, eosinophils and platelets [24]. Most of the IgE produced is bound to FCεRI on mast cells and basophils, where it is inert until target antigen binds IgE and crosslinks the receptor complex [9]. Cross-linking of the IgE complex on mast cells and basophils result in the degranulation of these cells and the release of local inflammatory mediators, such as histamine, enzymes and cytokines [8,9]. The release of these mediators is beneficial for parasite-specific immunological response (one of the main function of IgE), and can play a role in initiating humoral memory and anti-tumor immune responses [8,25]. However, when IgE-mediated activation of basophils and mast cells is inappropriately triggered it can result in atopic conditions.

Under physiological conditions, serum IgE is found in extremely low concentrations, constituting only 0.05% of total immunoglobulin, making it the most tightly regulated immunoglobulin isotype. The requirement of this tight regulation is due to the numerous IgE-related diseases that can result from increased levels of IgE, including allergic asthma, rhinitis, conjunctivitis, atopic eczema, and food and respiratory allergies [25].

1.2.1 Mechanisms regulating the IgE response

CSR is highly regulated and it only takes place when specific signals are present. These specific signals come from cytokines that bind to cell-surface receptors and promote the activation of positively acting transcription factors on B cells [8,9,13]. Depending on the cytokines, different transcription factors are activated, determining which antibody isotype will be produced. For CSR towards IgE, IL-4 and IL-13 are the most important cytokines [9,13]. As IL-4 and IL-13 production is largely restricted to Th2 T cells, IgE production by B cells is critically dependent on Th2 differentiation and effector function [13,25,26]

In newly activated B cells, signaling from IL-4 and IL-13 receptors synergizes with signaling from CD40 (in response to CD40L engagement), leading to the activation of transcription factors that interact with and activate the epsilon switch promoter [13], namely Stat6 [27,28], NF-κB [29], Pax5 [30], Pu1 [31], C/EBP [32], Ap1 [33] and E2A [34]. In addition, the expression of activation induced cytidine deaminase (AID) is induced by downstream signaling of these transcription factors [33], aiding the DNA rearrangement process for isotype switching [11,13]. These molecular interactions are represented in Figure 2.

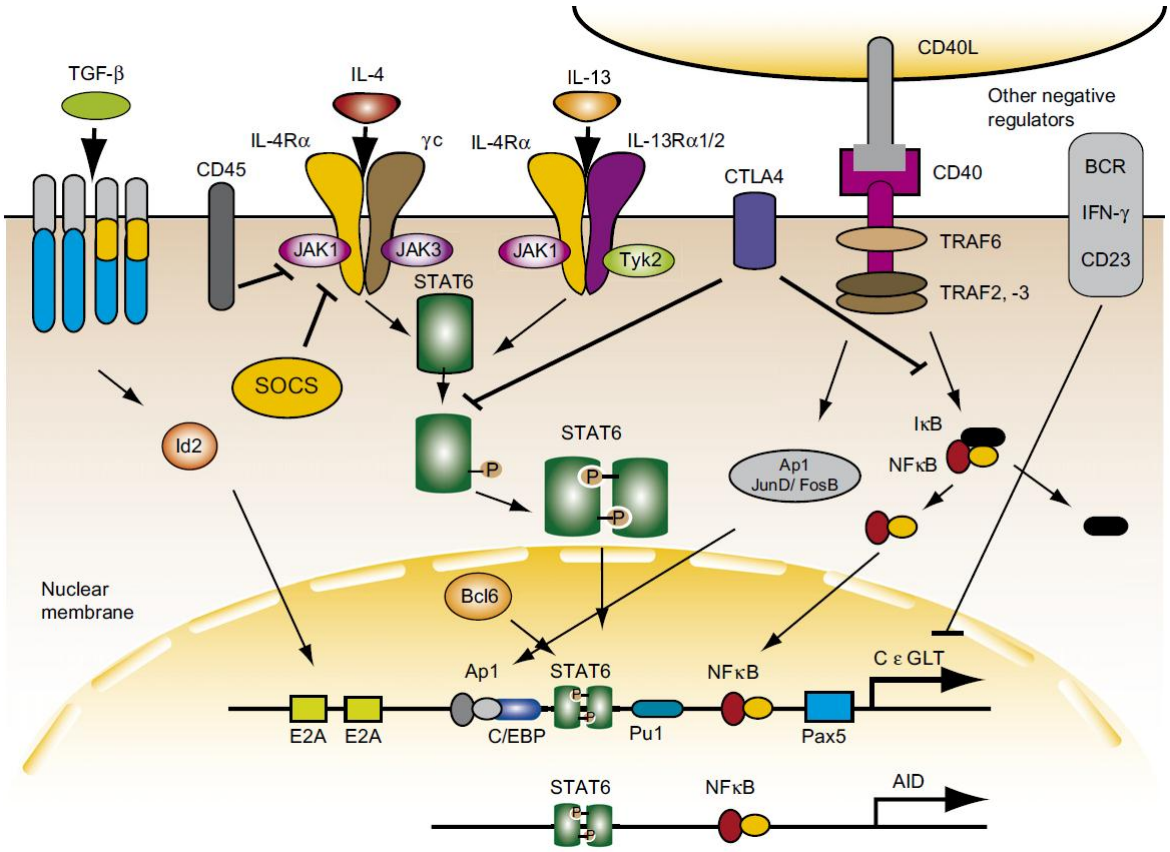

Figure 2 – Regulation of IgE CSR. Membrane signaling and molecular interactions that lead to the negative or positive regulation of IgE CSR [13].

Studies in *Stat6* KO mice raise the importance of STAT6 in the regulation of CSR to IgE, since levels of IgE are reduced or undetectable in these mice [27,28]. Normally, STAT6 is located in the cytoplasm as a dormant inactive transcription factor, which is activated by phosphorylation after stimulation with IL-4 and IL-13, leading to its dimerization and subsequent migration to the nucleus. These observations suggest, therefore, that STAT6 is the master regulator of CSR to IgE [8,13]. In order to regulate the action of this activators of transcription, transcription factor compete for the same binding sites, namely STAT6 competing with Bcl6 and E2A, with Id2, making the CSR event dependent on the balance of transcription factor inputs [13]. Studies on *Bcl6* KO mice show an increase in IgE production after IL-4 stimulation, accompanied by a lack of germinal centers, and the presence of multi-organ inflammation and IgE^+ B cells [35]. As mentioned before, *Stat6* KO mice have a reduction or complete absence of IgE. Double KO mice for Bcl6 and *Stat6* have the same phenotype as *Bcl6* single KO but with no population of IgE^+ B cells [35]. This demonstrates that Bcl6 modulates Stat6 function and consequently, the regulation of IgE immune response [35].

Similar to the effect of Bcl6 loss, in studies with *Id2* KO mice observe an increase in CSR to IgE and IgE positive B cells. Additionally, these mice lack lymph nodes and Payer's patches and show a large reduction in NK cells [36]. ID2 inhibits E2A interaction with E1 and E2 boxes of the GL ε promoter and therefore IgE CSR, in response to TGF-β1 [34]. Apart from Bcl6 and TGF-β, acting through ID2, other factors contribute to the regulation of IgE class switching [13]. Among them are CD45 [37,38], SOCS [39], CTLA4 [40], BCR [41], IFN-γ [42] and CD23 [43,44].

In addition to the complex regulation of isotype switching to IgE (which limits the number of B cells that can become IgE-secreting), IgE is also tightly regulated at multiple downstream stages. At the gene expression level, the process of alternative polyadenylation restricts mIgE expression, which results in a lower rate of matured mRNA production and diminished stability and in turn lower mIgE- based BCR representation and death of IgE producing cells [8,23]. Additionally, serum IgE has a short half-life and, after production, is rapidly bound by the high-affinity FcεRI on the surface of effector cells (where it acquires a long half-life time) [23]. As a result of these multiple processes negatively regulating IgE immune responses, the generation of IgE is slow and limited [23].

1.3 Hyper-IgE Syndrome

Elevated levels of serum IgE are commonly associated with allergies and parasitic infections, but other pathologic conditions are also characterized with high levels of IgE in the serum. Of these, the primary immune deficiencies are of particular importance due to the severity of disease. Primary immune deficiencies that can include elevated IgE production include, Olmsted syndrome[45], ADA deficiency[46], Wiskott- Aldrich syndrome, ALPS-II, DiGeorge syndrome, IPEX, Omenn syndrome, Ichthyosis vulgaris, Netherton disease, ZAP-70 deficiency and HIES [9,25,47,48], which is the focus of this work.

HIES, originally named Job's syndrome after the biblical prophet said to suffer from severe dermatitis with "cold" abscesses, was first defined in 1966 [49–51]. Latter, the syndrome was redefined after the detection of extremely elevated levels of serum IgE and other cutaneous manifestations and respiratory infections, and was included in the group of primary immunodeficiency diseases [49–51]. HIES is a complex immune pathology with diverse clinical manifestations and genetic heterogeneity [51], based on

which two forms of this syndrome can be recognized, Autosomal Dominant HIES (AD-HIES), caused by mutations in signal transducer and activator of transcription 3 (*STAT3*), and Autosomal Recessive HIES (AR-HIES), caused by dedicator of cytokinesis 8 (*DOCK8*) and tyrosine kinase 2 (*TYK2*) mutations. Many cases of HIES syndrome defined by clinical presentation remain without genetic diagnosis, suggesting the involvement of alternative, as yet unknown, genes.

1.3.1 Symptomatology

Both AD-HIES and AR-HIES are characterized by a classic clinical triad, including recurrent staphylococcal "cold" abscesses, afebrile airway infections and high levels of serum IgE (>10.000 IU/mL) [48]. However each form of HIES has a panoply of other physiological signs, which are described below.

1.3.1.1 AD-HIES

AD-HIES is a multisystem disease, which encompasses both immunologic and distinctly non-immunologic abnormalities. Non-immunologic characteristics include, defects in facial features, such as rough porous skin, asymmetric face, prominent shin and forehead, increased interalar distance and arched palate, delayed exfoliation of primary teeth, and abnormal development and bad quality of permanent teeth [51,52], musculoskeletal complications, such as degeneration of joint tissue at young ages and fragile bones, ophthalmologic problems, cranial malformation and vascular complications, comprising aneurysms, lacunar infarctions and hypertension [48–52]. Resembling several other primary immune pathologies, AD-HIES patients have a higher susceptibility to develop Hodgkin's and non-Hodgkin's lymphoma, leukemia, and vulva, liver and lung cancers [49–51,53].

Immunologic manifestations start at or soon after birth, with a newborn rash consisting of eosinophilic pustules mostly localized on the face and scalp [49,50]. In most patients these rashes progress to an eczematoid rash, and recurrent boils caused by *Staphylococcus aureus* infections appear in early childhood[49,50]. In these patients *S. aureus* skin abscesses are atypical given that cardinal features of inflammation, i.e. heat, erythema and soreness, are absent, so they are referred to as "cold" abscesses [49,50]. Fungal infections of the skin are also common in HIES patients, namely mucocutaneous candidiasis, histoplasmosis and *Crytococcus neoformans* [50,51,53]. By contrast, viral infections with herpes simplex virus are not frequent [51].

In addition to the cutaneous manifestations, airway infections are also common. Similarly to skin infections, sinopulmonary infections are mostly due to *S. aureus* and less frequently *Haemophilus influenza* and *Streptococcus pneumonia* [48–51,53]. During *S. aureus* pulmonary infections purulent sputum is present but there is often a lack of systemic signs of inflammation [49]. Recurrent pneumonias are typically complicated by lung abscesses, bronchiectasis, pneumatocoeles and bronchopleural fistules. The damage in the bronchopulmonary parenchyma and the impaired remodeling of the lung tissue predisposes to colonization by opportunistic infections, such as *Pseudomonas aeruginosa*, *Aspergillus fumigatus*, *Pneumocystis jiroveci*, *Mycobacterium intercellulare* and *Nocardia* [48–51].

The major cause of death in these patients results from these opportunistic infections, namely *Pseudomonas aeruginosa* and *Aspergillus fumigatus* [54], and invasion of blood vessels by mold infections, which lead to life-threatening hemoptysis and/or disseminate to extrapulmonary sites of infections [49]

1.3.1.2 AR-HIES

The main difference between AD-HIES and AR-HIES, in terms of multisystem symptomatology, is that the latter does not show signs of skeletal, dental or facial abnormalities [51,53]. However various cases can present with neurological symptoms secondary to infections and vasculitis [49–51,53]. Facial paralysis, hemiplegia, ischemic infraction, and subarachnoid hemorrhages are common neurologic affectations and contribute to high mortality in AR-HIES [51].

As in AD-HIES, elevated IgE levels in the serum, eczema, recurrent bacterial skin infections, mucocutaneous candidiasis and pneumonias, in this case without formation of pneumatocoele, portray typical symptomatology in AR-HIES [49]. Particularly in AR-HIES, patients often suffer from recurrent otitis media, mastoiditis, sinusitis and bronchitis with bronchiectasis and autoimmune hemolytic anemia and cytopenias might occur [49–51,53]. AR-HIES patients differ from AD-HIES in their propensity to develop severe atopy, anaphylaxis and asthma [49–51,53]. Also, AR-HIES patients have defects in humoral immunity [55].

In addition to skin bacterial infections, AR-HIES patients also have chronic skin viral infections which are restricted to this form of the disease and are mainly caused by herpes simplex virus, human papillomavirus, molluscum contagiosum virus and varicella-zoster virus [49,50]. Respiratory infections are also typical to AR-HIES and are caused by *H. influenza*, *S. pneumonia*, *P. jiroveci*, *Histoplasma capsulum, S. aureus* and

Legionella pneumophila, and by respiratory adenovirus and syncytial virus [49,50]. As such, it is perhaps not surprising that sepsis is a major cause of death at early age [49].

Patients suffering from AR-HIES have a higher predisposition for early onset of malignancies, usually related to cutaneous viral infections, which is another major cause of death [51]. Such malignancies include squamous cell carcinoma, microcystic adnexal carcinoma, and several lymphomas [50].

1.3.2 Etiology

1.3.2.1 AD-HIES – Immunological implication of the disruption of signaling mechanisms due to STAT3 mutations

AD-HIES is caused by mutations in *STAT3*. STAT3 plays an important role in a great number of signaling pathways in diverse tissues [56]. Abnormalities in the regulation of these pathways due to dominant negative mutations in *STAT3* are reflected in the systemic complications that HIES patients present apart from the immunologic defects.

In the immune system, STAT3 plays a role in transduction signals from numerous cytokines, which control the expression of pro-inflammatory and anti-inflammatory proteins [52]. Among these are IL-6, IL-10, IL-21, IL-22, IL-23 [51], IL-11, IL-17, leukemia inhibitor factor, oncostatin M, cardiotrophin-1, cardiotrophin-like cytokine, ciliary neurotrophic factor [52]. The net effect of defective signaling through this set of cytokines in AD-HIES is a defect in Th1 and Th17 differentiation and skewing towards Th2 differenciation [51]. AD-HIES patients also reveal diminished memory T-cell populations, decreased delayed-type hypersensibility response, impaired response of lymphoid cells to antigenic and allo-antigenic stimulation [51] and defective neutrophil granulocyte chemotaxis, as seen by Hill et al in 1974 [57]. Each of these immunological phenotypes contributes to a subset of clinical phenotypes.

The defect in Th17 differentiation in AD-HIES is likely the key defect causing increased susceptibility to bacterial and fungal infections. Th17 cells absent in AD-HIES patients due to defective induction of the master transcription factor ROR- γt [58–60]. Th17 cells are critical for fighting infections of organisms such as *C. albicans* and *S. aureus*, as they are the primary source of IL-17 during an infection [58]. IL-17 initiates downstream pro-inflammatory signaling cascades, resulting in the expression of IL-8, IL-6 and G-CSF in non-immune cells, activation of neutrophils through regulation of G-CSF and its receptor, expression of acute phase proteins and molecules with

antimicrobial activity, like lipocalin2 and C-reactive protein, and β-defensins and mucins, respectively [61], which correlate with the persistent infections with *C. albicans* and *S. aureus* in AD-HIES patients. Additionally, IL-17 induces expression of the chemokine CCL20 that has chemotactic activity and recruits T cells and DCs to inflamed skin and mucosa, perhaps explaining the tissue-specificity of many AD-HIES infections.

In addition to the defect in Th1/Th17 immunity, a strong Th2 response is the hallmark of STAT3 deficiency. Increased numbers of Th2 cells, particularly in the absence of Th1-produced IL-12 and IFNγ (which limit Th2 activation) favor the production of IL-4 and IL-13 cytokines. As described above, these cytokines strongly influence the isotype switching of B cells into the IgE-producing lineage, which is then responsible for the increased serum IgE levels and the resulting atopic diseases [53].

$CD4^+$ T_{regs} are responsible for the maintenance of peripheral tolerance. They suppress effector T cell preventing exacerbated immune responses and autoimmunity. Under normal circumstances, exposure to allergens induces the production of IL-10, by local non-immune cells, which is detected by DCs that signal in favor of an allergen-specific tolerance, generating the formation of iT_{regs} [62]. Defects in STAT3 leads to a defect in IL-10 signaling which impairs the generation of tolerogenic DCs and formation of iT_{reg} [62–64].

1.3.2.2 AR-HIES – Immunological consequences of the disruption of signaling mechanisms due to DOCK8 mutations

AR-HIES can be caused by mutations in *DOCK8*. Lymphopenia is an important characteristic of DOCK8-deficiency and reflects the immunodeficiency observed in AR-HIES. Lymphopenia due to *DOCK8* mutation especially affects $CD4^+$ T cells [65,66], but $CD8^+$ T cells (naïve and memory) [67], NK cells [68] and B cells [55] are also frequently decreased. DOCK8 has a prominent role in T-cell activation, since the proliferative capability of both CD4 and CD8 T cell populations is diminished in DOCK8-deficient patients [69]. For example, in a study of 11 patients with DOCK8-deficiency it was observed that most of the patients had low cell counts for total T cells, CD4 T cells, CD8 T cells, low absolute numbers of T_{regs} but normal proportions, mild to moderate eosiniophilia, high levels of serum IgE and normal numbers of neutrophils and monocytes [65]. Some patients also had low numbers of NK cells and B cells [65]. Additionally, they tested the proliferation of $CD8^+$ T cells from activated PBMCs after

stimulation with IL-2 and observed that this population did not expand well [65]. The low counts of CD8 T cells and their impaired capability to proliferate may explain the incidence of human papillomavirus-related cancer in three of the patients [65] and the general susceptibility of AR-HIES patients to viral infections (a phenotype not observed in AD-HIES).

In a recent study, Lambe *et al*. (2011), Dock8-deficient mice were used to assess the immunological characteristics of DOCK8 deficiency in humans [66]. In this study, the authors report that mice and humans reveal lymphopenia, mostly due to decreases in the number of naïve T cells. Furthermore, a reduction of IFNγ- and TNFα-producing cells and a higher proportion of IL-4-secreting cells were observed under Th1 and Th2 polarizing conditions, respectively [66]. Additionally, Dock8-deficient mice, although able to produce a normal primary immune response to viral immunization, had a significant reduction in the memory response due to decreased survival of $CD8^+$ T cells.

To further understand the role of DOCK8 in $CD8^+$ T cells Randal *et al*.(2011) analyzed both mice and patients with Dock8/DOCK8 deficiency [67]. In this study the authors detected a highly significant loss of naïve cells, along with a smaller but still significant decrease in memory cells within the $CD8^+$ T cells compartment. Additionally, most of the $CD8^+$ T cells of the patients had a phenotype ($CD45RA^+CCR7^-$) associated with cellular exhaustion or replicative senescence and were unresponsive to CD3/CD28 stimulation. The authors demonstrate that the defect in memory CD8 T cell persistence, observed not only in this study [66], involved the failure in recruitment of LFA-1 to the CD8 T cell synapse with DCs. Antiviral defense is dependent on a fully functional population of CD8 T cells [70] suggesting that these studies reporting a defect in memory and naïve CD8 T cells may explain the chronic persistence of the viral infections in the DOCK8-deficient patients [71]. Defective cytotoxicity of NK cells may also contribute to impaired viral clearance [68]. The difficulty in controlling viral infections of the skin, and not systemically, is a typical characteristic of AR-HIES patients with *DOCK8* mutations and it may suggest additional defects in local antiviral immunity within the skin [71] or a defective chemotactic signaling which prevents an adequate migration of lymphocytes towards the skin, during infections [70].

In B cells, DOCK8 is required for the formation of the immunological synapse by recruiting ICAM-1 and, especially in GC B cells, to promote survival and selection during the affinity-maturation phase of GC response [55]. *DOCK8* mutations damage this

process affecting the longevity and affinity maturation of T cell-dependent antibody responses and the antigen-recognition due to the malformation of the immunological synapse [55].

The role DOCK8 plays in cytoskeletal organization, it may be the reason patients with deficiencies in this protein show impaired T-cell activation and effector responses [69]. Additionally, the maintenance of memory Th17 appears to be affected in DOCK8-deficient subjects [69]. The deficiency in Th17 may also reflect a more widespread derangement of Th-cell differentiation [69].

1.3.2.3 AR-HIES – Immunological consequences of the disruption of signaling mechanisms due to TYK2 mutations

Unlike *STAT3* and *DOCK8*, *TYK2* has not been described as having non-immunologic functions. In the study by Minegishi, *et al.* (2006) which reports the identification of *TKY2* as the genetic foundation in a patient clinically diagnosed with HIES, systemic affectations are not described [72].

In addition to mutations in *DOCK8*, AR-HIES can also be caused by loss-of-function mutations in *TYK2*. In TYK2-deficient patients, the response to type 1 IFN, IL-6, IL-10, IL-12 and IL-23 are impaired, a defect which can be reversed by restoring a functional copy of TYK2 [72–74]. The functional role of TYK2 is less well understood than STAT3 or DOCK8, as *Tyk2* KO mouse do not show the same phenotype, impeding the use as a model [72,74]. Nevertheless, *TYK2* mutant cells show defective STAT4 activation and hence imped Th1 differentiation [74]. By contrast, Th2 differentiation is dramatically enhanced [72], and thus, as in *STAT3* and *DOCK8* patients, the hyper-IgE production in *TYK2* patients is likely driven by excessive IL-4 and IL-13 secretion by Th2 cells.

Similarly to defects in STAT3, deficiencies in TYK2 compromise IL-10 impairing the formation of DCs and iT_{regs} [62–64] and leading to a defective regulation of Th2 cells by $T_{regs,}$ which in turn promote the emergence of the atopic phenotype [75], typical of these patients.

1.3.2.4 Diagnosis of HIES

The diagnosis of HIES is given to a patient using a scoring strategy, in which several typical parameters present in the patient are scored and summed. When the score is 60 or greater the patient is given the definitive diagnosis of HIES [76]. The parameters used to score HIES were defined by Grimbacher, *et al.* [76] and are described Table 1.

Table 1 – Scoring system of the clinical features of HIES patients.

Points Clinical Findings	0	1	2	3	4	5	6	7	8	10
Highest serum-IgE level (IU/ml)	<200	200-500			501-1000				1001-2000	>2000
Skin abscesses	None		1-2		3-4				>4	
Pneumonia (episodes over time)	None		1		2		3		>3	
Parenchymal lung anomalies	Absent						Bronchiectasis		Pneumatocele	
Retained primary teeth	None	1	2		3				>3	
Scoliosis (maximum curvature)	<10°		10-14°		15-20°				>20°	
Fractures with minor trauma	None				1-2					
Highest eosinophil count (cell/µL)	<700			700-800			>800			
Characteristic face	Absent		Mildly present			Present				
Midline anomaly	Absent					Present				
New born rash	Absent				Present					
Eczema (worst stage)	Absent	Mild	Moderate		Severe					
Upper respiratory infections (per year)	1-2	3	4-6		>6					
Candidiasis	None	Oral	Fingernails		Systemic					
Other serious infections	None				Severe					
Fatal infection	Absent				Present					
Hyperextensibility	Absent				Present					
Lymphoma	Absent				present					
Increased nasal width	<1 SD	1-2 SD		>2 SD						
High palate	Absent		Present							
Young-age correction	>5			2-5 years				≤1 year		

Adapted from Grimbacher, *et al.* [76]

1.3.3 Treatments

A cure for HIES, either in the autosomal dominant or autosomal recessive form has not been found yet, so therapeutic strategies focus on the prevention and management of infections [51,53]. Common therapies to both forms of the disease include prophylactic antibiotic treatment against staphylococcus, to reduce skin abscesses and pneumonias [53]. High doses of intravenous antibiotics for a prolonged time are required to eliminate infectious agents at regular intervals. In addition to systemic antibiotic treatment, the use of antibacterial, moisturizing creams and topical steroids are recommended [53]. Taking bleach baths and swimming in chlorinated pools has been found to decrease colonization by *S. aureus* [50]. For the treatment of mucocutaneous candidiasis, oral triazole antifungals is preferred [53]. Lung abscesses may need surgical intervention, which carries high risks [51].

Cyclosporine A and intravenous Ig infusion therapy (IVIG) have been used successfully [53]. IVIG may influence the IgE levels due to an increase in Ig catabolism or IgE neutralization via an anti-idiotype network [53]. As integrity of antibody formation, especially against encapsulated organisms, appears to be impaired in HIES, the use of IVIG is reasonable to consider to prevent infections as well [53].

Additional treatments are advised based on the subtype of HIES. Specifically for AD-HIES aggressive treatment of pneumonias is applied to prevent parenchymal lung damage and bronchoscopy is performed to isolate the causative pathogen and remove pus [49].

By contrast, in AR-HIES, hematopoietic stem cell transplantations, although not a standard care, can function as definitive treatments. However, they must be used with caution due to the normal risks associated with transplantation as well as an increased risk of viral infections which are already difficult to control after transplantation [50].

1.3.4 Genetics

STAT3, *DOCK8* and *TYK2* have been identified as genes in which mutations can drive HIES. However, it is likely that mutations in other genes are also able to cause HIES, as multiple other genes have been associated with IgE regulation in both humans and mice (Table 2). These additional genes fall in several main classes: i) Mendelian mutations that cause elevated IgE in patients in diseases not considered HIES due to additional clinical presentations (eg. *FLG*[77,78] and *FOXP3*[25]); ii) genes with polymorphisms associated with elevated IgE in genome-wide association studies

(GWAS) of patients, but with no Mendelian mutations identified (eg. *RAD50* [79] and *HLA-DRB1* [80]); and iii) and gene where Mendelian mutations have been identified to cause HIES-like diseases in mice, but where no human mutations have yet been identified (e.g. *Card11*) [81–83]

Table 2 – Genes associated with IgE production.

Gene	Species	Association	Ref	Gene	Species	Association	Ref	Gene	Species	Association	Ref
ADA	Hu	Mendelian	25	*FLG*	Hu/Mu	Mendelian	77,78	*RAD50*	Hu	GWAS	79
Card11	Mu	Mendelian	76–78	*FOXP3*	Hu	Mendelian	25	*RAG1*	Hu	Mendelian	25
CASP10/ Casp10	Hu/Mu	Mendelian	25	*HLA-DRB1*	Hu	GWAS	80	*RAG2/ Rag2*	Hu/Mu	Mendelian	25
Cbl	Mu	Polygenic	84	*Icos*	Mu	Polygenic	25	*RMRP*	Hu	Mendelian	25
CCL11	Hu	Polygenic	25	*Id2*	Mu	Mendelian	34	*SPINK5*	Hu	Mendelian	25
CCL26	Hu	Polygenic	25	*IFNγR*	Hu	Polygenic	25	*SPP1*	Hu	Polygenic	25
Ccr3	Mu	Polygenic	25	*IL-13*	Hu	Polygenic	25	*STAT3*	Hu	Mendelian	25,85
CD14	Hu	Polygenic	25	*Il-21*	Mu	Mendelian	25	*STAT6*	Hu	GWAS	25
CD23	Mu	Polygenic	86	*IL-2R*	Hu	Polygenic	25	*Tcra*	Mu	Polygenic	25
CD274	Hu	Polygenic	87	*IL-4*	Hu	Polygenic	25	*TNF*	Hu	Polygenic	25
CD28	Hu	Polygenic	87	*IL-4R*	Hu	Polygenic	25	*TNFSF18*	Hu	Polygenic	87
CD40	Hu	Polygenic	25,87	*IL-7RA*	Hu	Mendelian	25	*TNFSF4*	Hu	Polygenic	87
CD80	Hu	Polygenic	87	*Lat*	Mu	Polygenic	25	*TRPV3*	Hu	Mendelian	45
CD86	Hu	Polygenic	87	*Lcp2*	Mu	Polygenic	25	*TYK2*	Hu	Mendelian	25,85
CTLA4	Hu	Polygenic	87	*LILRA4*	Hu	Polygenic	87	*VTCN1*	Hu	Polygenic	87
DCRLE1C	Hu	Mendelian	25	*MS4A2*	Hu	Polygenic	25	*WAS/ Was*	Hu/Mu	Mendelian	25
DOCK8	Hu	Mendelian	25,85	*NOD1*	Hu	Polygenic	25	*Wip*	Mu	Polygenic	25
Fas	Mu	Mendelian	25,88	*PAFAH*	Hu	Polygenic	25	*ZAP-70/ Zap-70*	Hu/Mu	Mendelian	25
FCER1A	Hu	GWAS	25	*PHF11*	Hu	Polygenic	25				

Genes are represented on their abbreviated form. Hu/Mu indicates genes identified in humans/mice, respectively. Ref. is the reference where the association with elevated levels of IgE is described

1.4 CARD11

CARD11, caspase recruitment domain family member 11, is also known as *BIMP3* or *CARMA1*. *CARD11* is a long gene with near 380kb of length and 25 exons, which code for a 4kb transcript and a protein with 1154 amino acids. It has 4 known

splicing variants, 3 of which are protein coding. CARD11 is a scaffolding protein that belongs to the membrane-associated guanylate kinase (MAGUK) family. CARMA1 is expressed only in the immune system and mediates downstream events of TCR and BCR signaling leading to the activation of NF-κB. Activation occurs via the destabilization of the inhibitory conformation of CARD11, producing the activated conformation. Activated CARD11 then recruits Bcl10 and MALT1 to the lipid rafts forming the CARD11-Bcl10-MALT1 (CBM) complex. This complex in turn activates IκB kinase (IKK), which phosphorylates IκB allowing the release of NF-κB. Finally, released NF-κB enters the nucleus, where it promotes the transcription of various genes, mediating the transcriptional effect of the CARD11 (Figure 3) [89].

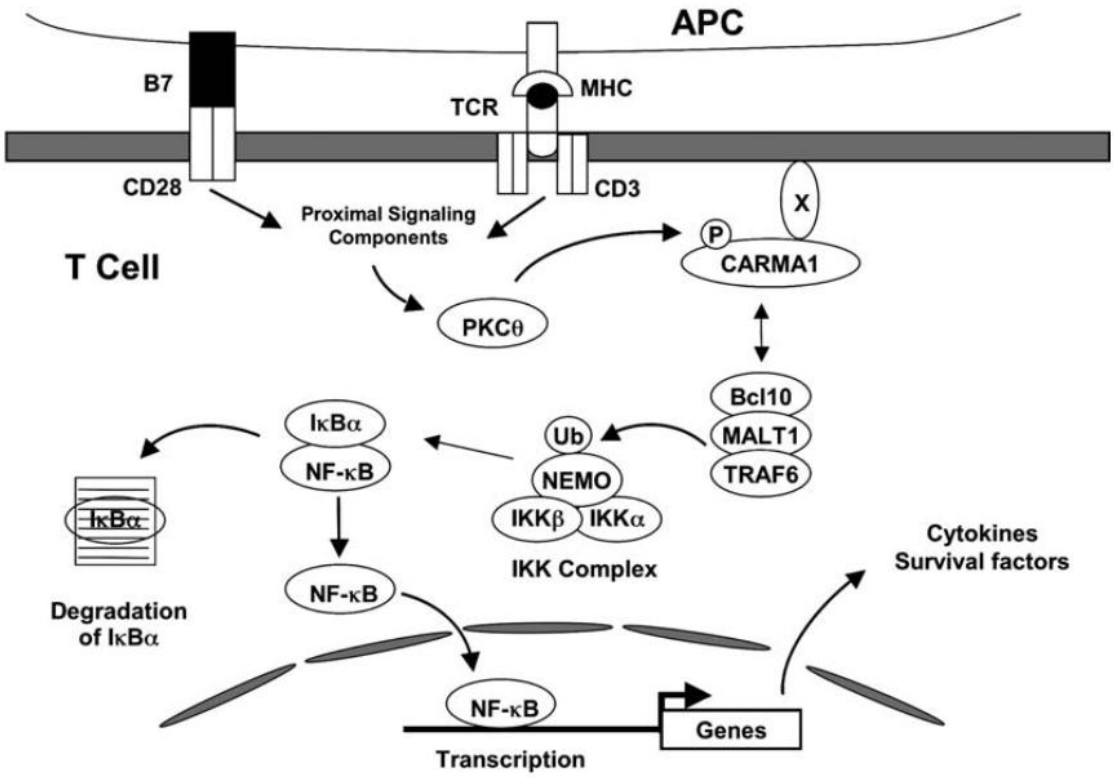

Figure 3 – CARD11 signaling in T cells [89]. Interaction of CD28 and TCR with APC molecules induces the activation of PKCθ, which phosphorylates CARD11 (CARMA1). CARD11 recruits Bcl10 and MALT1 complex and activates TRAF6 later on, which promotes the ubiquitination and activation of the IKK complex. In turn, the functional IKK complex activates NF-κB, which migrates into the nucleus and promotes the transcription of several genes [89].

Studies using *Card11* knockout mice show that the intact function of Card11 is required for the differentiation of NK cells, the differentiation and activation of B cells and the activation of T cells [90]. The key role of Card11 in T cell activation lies in signal transduction of TCR/CD28 stimuli for activation. However additional roles also exist

for Card11 in Th2 cells, Th17 cells and T_{regs}. For Th2 cells, Card11 is required for the induction of Th2 master transcription factors GATA3 and JunB (which promote the differentiation of Th2 cells), and also the production of key effector molecules IL-4 and IL-10 [82]. Mice overexpressing *Card11* have a Th2-cell mediated inflammatory phenotype [82].

In the particular case of Th17 cells, Card11 is not only necessary for their differentiation but also for modifying the chromatin context of Th17 effector genes to allow transcription [91]. In the case of T_{regs}, decreased expression of *Card11* compromises the formation of T_{regs}, which are found to a lesser extend in the periphery and in the thymus compared to wild-type mice [83]. This contrasts with what is observed in *Card11*-knockout mice, in which the presence of T_{regs} is abolished [83].

In humans, CARD11-deficiency has been associated with immune deficiency. Reports in consanguineous families describe *CARD11* homozygous loss-of-function mutations resulting in a decrease in NF-κB activation and combined immune deficiencies [92,93]. This phenotype mirror loss-of-function mutation in *Card11* in mice [90], however, partial loss-of-function mutation in *Card11* in mice have a more complex phenotype, combining immune deficiency with elevated levels of IgE and Th2 cell-associated inflammation [81,82,94]. These results suggest that hypomorphic alleles of *CARD11* may be associated with combined immunodeficiency and hyper-IgE in humans, however, such patients have not yet been described.

2 Hypothesis and aims

A Belgian family was identified with two individuals diagnosed with atypical HIES. Prior to the initiation of this project, the known Mendelian HIES genes (*DOCK8*, *STAT3* and *TYK2*) were tested and no mutations associated with this disease were found. The hypothesis of the current project is that HIES in this family is a Mendelian inherited disorder caused by mutations in novel HIES genes.

In order to investigate this hypothesis we aim to:

1. Examine the clinical and immunological phenotype of Patient 2 to identify putative mechanistic pathways of disease development
2. Identify candidate genes for disease causation by cross-referencing all-exome sequencing data of Patient 1 to the known literature on IgE regulation in humans and mice
3. Test candidate genes for a role in HIES causation by the investigation of inheritance pattern and functional testing.

3 Methodology

3.1 Peripheral Blood Mononuclear Cell (PBMC) isolation

The study was approved by the Ethics Committee of UZ Leuven and written informed consent was obtained from the patients, parents and siblings. Blood was drawn from each donor only after informed consent had been given. All healthy controls used were clinically disease-free, were matched for sex and age to all the family members and also gave informed consent. The patients are a female born in 2010 and a male born in 2007 which were included in the study when they were 1 and 3 years old, respectively. The patients are born from consanguineous, healthy parents (the mother was 34 years old and the father was 49 years old) and siblings to two healthy children, one girl with 7 years of age and one boy with 9 months (analysis was done on samples collected from the patients and family members when they were included in the study except when referred otherwise).

Blood from patients, family members and controls was collected in the pediatric ward at Gasthuisberg, UZ Leuven using heparin tubes. Approximately 25mL of blood was collected from each individual. Aliquots of whole blood and plasma were prepared and kept at -80º C. The remainder of the collected blood was subject to a density-gradient centrifugation using MP Biomedicals LSM* Lymphocyte Separation Medium (Fisher Scientific, Hampton, New Hampshire, U.S.A.) in order to separate different components of the blood. Blood was placed directly above the LSM in a proportion of 2:1 (two parts of blood: one part of LSM) and centrifuged at 400g for 25 minutes at 18°C with no break or acceleration. PBMCs were collected from the interphase located directly above the LSM. PBMCs were counted using the cell counter Countess (Life Technologies, Carlsbad, California, U.S.A.) and divided in aliquots of approximately 40 million cells and stored at -80º C in freezing medium (90%FBS+10%DMSO) and approximately 2 million cells in 1mL TRIzol® Reagent (Life Technologies, Carlsbad, California, U.S.A.).

3.2 DNA and RNA extraction

Genomic DNA was extracted from one vial of whole blood using the QIAamp DNA Blood Midi Kit (Qiagen, Venlo, Netherlands) using the following procedure. 1.8mL of whole blood was added to Protease solution, mixed in Buffer AL and incubated at 70°C for 10 minutes to lyse the cells. After cell lysis, absolute ethanol was

added to promote the binding of the DNA to the column. The mixture was then added to the column and centrifuged at 3000rpm for 3 minutes. The filtrate was discarded and a washing step was performed adding Buffer AW1 to the column and centrifuging at 5000rpm for 1 minute. Filtrate was discarded and a second washing was performed by adding Buffer AW2 to the column and centrifuging at 5000rpm for 2 minutes. Collection tube with filtrate was discarded and column was placed in a new collection tube. Elution was performed by adding Buffer AE to the column, incubating for 5 minutes and centrifuging at 5000rpm for 2 minutes.

From samples stored in TRIzol DNA and RNA was extracted. Chloroform was added to the TRIzol, incubated 10 minutes at room temperature (RT) and centrifuged at 13000rpm for 15 minutes at 4°C. As a result of this step 3 phases became evident: an upper phase containing the RNA, an interphase with DNA, and an organic phase. The upper phase with the RNA was carefully removed. The organic phase and interphase were kept for DNA extraction. The DNA extraction was performed by adding absolute ethanol to the organic phase and centrifuging at 2000xg for 5 minutes at 4°C to obtain a DNA pellet. The pellet was then washed twice with a solution of 0.1M of sodium citrate with 10% ethanol and at each wash, an incubation for 30 minutes at RT and a centrifugation at 2000xg for 5 minutes at 4°C was performed. The pellet was then washed in 75% ethanol centrifuged at 2000xg for 5 minutes at 4°C, ethanol was discarded and the pellet air dried. The pellet was then dissolved in DNase-free water.

In order to obtain RNA with higher quality both TRIzol and Allprep DNA/RNA Mini Kit (Qiagen) were used in the same procedure as follows. To the upper phase one part of 70% ethanol was added and the mixture was placed in the RNeasy mini column and centrifuged at 10000rpm for 15 minutes. Flow-through was discarded and Buffer Rw1 was added to the column and centrifuged for 15 minutes at 100000rpm for the first washing step. The flow though was discarded and a second washing step was performed with Buffer RPE using the same centrifugation settings as in the previous washing. Flow-through was discarded and a final washing step was done with the Buffer RPE and centrifuged for 2 minutes at 10000rpm. The flow-through was discarded and a dry centrifugation was done for 1 minute a full-speed to remove ethanol residues. The column was then placed in a new tube and the RNA eluted in RNase-free water by incubating for 3 minutes at RT and centrifuging for 1 minute at 10000rpm.

RNA and DNA concentrations were quantified using the Nanodrop 2000 (Thermo Scientific, Waltham, Massachusetts, U.S.A.).

3.3 Genetic analysis

Full exome sequencing of Patient 1 was performed on 10 µg of DNA by the Beijing Genomics Institute (BGI)-Hong Kong. The sequencing was performed using the Illumina Hiseq2000 platform (Illumina, California, U.S.A.), on a library of enriched exome-fragments as previously described[95]. Three micrograms of purified genomic DNA were randomly fragmented by ultrasonoscope (Covaris, Massachusetts, USA) to generate 150~200bp fragments. The shotgun library was subsequently hybridized to Agilent SureSelect Human All Exon v2 kit (44 Mb) (Agilent Technologies,California,USA) for exome enrichment and subjected to rounds of amplification before quality check with 2100 Bioanalyzer (Agilent Technologies) and quantification by quantitative RT-PCR with StepOnePlus Real-Time PCR System (Life Technologies, California, USA). The quantified library was analyzed by an Illumina Hiseq2000 platform (Illumina, California, USA) with 90bp paired-end reads. Adaptor-containing reads and low quality reads (defined as reads containing 50% or more bases with a quality value <5) were discarded for quality control. High quality reads were aligned to the human reference genome (hg19) with SOAPaligner (version 2.21)[96]. Duplicated reads and reads with alignment length < 75bp were excluded from SNP calling. SOAPsnp (version 1.05) [97] was used to generate genotypes. For SNP quality control, low quality SNPs that meet one of four following criterions were filtered out: (i) Genotype quality < 20; (ii) sequencing depth < 4; (iii) estimated copy number is > 2; (iv) distance from the adjacent SNPs < 5bp. Small Indel detection was performed using the UnifiedGenotyper tool from GATK (version v1.0.4705) [98] after all the high quality reads were aligned to the human reference genome using BWA (version 0.5.9-r16) [99]. Detected variants were filtered to remove those which were non-exonic, synonymous or non-rare (allele frequency greater than 0.5% in dbSNP, 1000 Genomes, HapMap or YH).

Large sample SNP typing was performed in collaboration with Professor Dieter Lambrechts, KU Leuven, using Sequenom technology. 100ng/µL of genomic DNA with a A260/280 superior to 1.85 were analyzed in a blinded manner using iPLEX technology on a MALDI-TOF based MassARRAY Compact Analyzer (Sequenom Inc., California, U.S.A.) as previously described [100].

Alternative detection of the presence/absence of mutations was performed via Sanger Sequencing, using gDNA prepared as per section 3.23.2. Specific primers (Table 4) were designed, using Primer3Plus software [101], for the *CARD11* variants and

reactions were run using GoTaq® Flexi DNA Polymerase (Promega, Fitchburg, Wisconsin, U.S.A.) and specific reverse and forward primers (IDT). Per reaction was used 1x Green GoTaq® Flexi Buffer, 1mM MgCl2, 0,2mM dNTP (Thermo Scientific), 0,4mM PrimerMix, 1,25U GoTaq® DNA Polymerase, water and ~100ng of cDNA or gDNA to a final volume of 25µl. The reaction was performed in T100™ Thermal Cycler (Bio-Rad, Hercules, California, U.S.A.) with an initial denaturation at 95ºC for 2 minutes, 35 cycles of denaturation at 95ºC for 20 seconds, annealing at 57ºC for 30 seconds and extension at 72ºC for 50 seconds or 1 minute, for cDNA and gDNA respectively, and a final extension at 72ºC for 5 minutes. Amplification was detected via running the reaction samples on a 2% agarose gel. The remaining PCR product was treated with USB® ExoSAP-IT® PCR Product Cleanup (Affymetrix®, Santa Clara, California, U.S.A.) accordingly to the manufacturer's instructions. The PCR product and the specific reverse primer used in the PCR reaction were then sent for Sanger sequencing by the VIB Genetic Service Facility, University of Antwerp or Laboratory of the Government Chemist Genomics, Berlin, Germany.

The prediction of alterations on the protein structure and function caused by the mutation was performed using the bioinformatic tools Polyphen-2 v2.2.2 [102] and SIFT [103].

3.4 Gene expression analysis

Following mRNA purification from patients and healthy family members (section 3.2), mRNA was converted to complementary DNA (cDNA) using the SuperScritp®III First-Strand Synthesis SuperMix and both oligo(dT) and random-hexamers, as such: 1µl of oligo(dT), 1µl of random-hexamers, 1µl of annealing buffer, up to 5µg of total RNA and RNase/DNase-free water for a total volume of 8µl. This mix was incubated at 65°C for 5 minutes and then immediately placed on ice. 10µl of 2x First-strand reaction mix and 2µl SuperScript®III/RNaseOUT™ Enzyme mix were added and incubated 10 minutes at 25°C, followed by 50 minutes at 50°C and finally 5 minutes at85°C. To measure the relative levels of gene expression in the cDNA samples, Power SYBR® Green PCR Master Mix was used in the following conditions: a total volume of 10µl per reaction containing as final concentration 1x Power SYBR® Green PCR Master Mix, 100 nM of forward and reverse primers (Table 4) and 5ng of cDNA. The PCR reaction was run on StepOnePlus™ Real-Time PCR Systems and StepOne Software v2.1 (Applied Biosystems) using the following program:

- PCR amplification: 10 minutes at 95° C, 50 cycles of 15 seconds at 95° C and 1 minute at 60° C
- Melting curve: 15 seconds at 95° C, 1 minute at 60° C and 15 seconds at 95° C

Primer combinations were tested using the GoTaq® Flexi DNA Polymerase (Promega) and gel electrophoresis. After qPCR was performed the molecular weight of the amplicons was confirmed by gel electrophoresis.

Relative gene expression of *CARD11* and *IL-4* was normalized to the average of expression of β-actin, GAPDH and HPRT. Expression of *CARD11* and *IL-4* in the patients was compared to the expression in healthy individuals. Specific primers were used for each housekeeping gene (Table 4).

3.5 Cloning-based allele-specific expression assay

Genomic DNA and cDNA of both patients and healthy family members were prepared as per sections 3.2 and 3.4. The target sequence surrounding the *CARD11* SNP was amplified from cDNA and gDNA of the patients and healthy family members using PCR and specific primers (Table 4). The PCR was prepared as per section 3.3. The PCR product from the cDNA had a molecular weight of 506bp, while the PCR product generated from gDNA was 698bp.

Following the generation of PCR products, the band with the correct size was excised from a 2% agarose gel and purified using the MinElute® Gel Extraction Kit (Qiagen) following the manufacturer's instructions. Following purification, the amplicon was cloned into the pCR®2.1-TOPO® Vector (Invitrogen). For the cloning reaction the TOPO®TA Cloning® Kit pCR®2.1-TOPO® Vector (Invitrogen) was used accordingly to the manufacturer's instructions mixing 1µl of Salt Solution, 1µl of pCR®2.1-TOPO® Vector, 2µl of purified PCR product and 2µl of water, and incubated 30 minutes at 22.5°C. The vector was then transfected to One Shot® TOP10 Competent Cells (Invitrogen). The transfected bacteria were then plated in Lysogenic Broth (LB) agar plates supplemented with ampicillin and incubated over night at 37ºC.

At least 60 colonies from each sample were used for the allele-specific quantification. As the colonies being added as template in the PCR, back up plates were made. To test for transfection with an amplicon-containing vector, a PCR was prepared with the same components as the PCR before the cloning except that the 1x Colorless GoTaq® Flexi Buffer was used instead of the 1x Green GoTaq® Flexi Buffer and using

a single colony as template for each reaction. The reaction was performed with an initial denaturation at 94ºC for 10, 35 cycles of denaturation at 94ºC for 2 minutes, annealing at 57ºC for 1 minute and extension at 72ºC for 1 minute, and a final extension at 72ºC for 5 minutes. The presence of the insert was confirmed by running the PCR product in a TBE gel with 2% agarose (GeneMate).

After confirming that the colonies incorporated the insert, each colony was genotyped using a SNP Genotyping Assay (Applied Biosystems, Foster City, California, U.S.A.). The assay was prepared using 1x TaqMan® Universal PCR, 0.5x Assay Mix, water and 1µl of PCR product to a total volume of 5µl. The conditions used for the reaction were an initial step of 10 minutes at 95º C and 35 cycles of denaturation for 15 seconds at 92º C and annealing/extension for 1 minute at 60º C. The real time PCR was run in an optical 96-well reaction plate using a 7300 Real Time PCR System and the 7300 System SDS software (Applied Biosystems). The Assay Mix was supplied as 40x and contained a set of PCR primers specific for the sequence and two TaqMan® MGB probes, one specific for each allele. The common allele was labeled with VIC® and the variant allele was labeled with FAM™.

3.6 Flow cytometry

PBMCs of Patient 2 (at the age of 6) and 36 age-matched (2-16 years old) healthy controls were isolated as described in 3.1 and were stained with anti-human antibodies, as listed on Table 3. For surface staining, cells were blocked for 20 minutes with blocking buffer, stained for 35 or 45 minutes (depending on the staining set) and fixed for 30 or 20 minutes on ice (depending on the staining set). Between each step two washing steps were done using FACS wash buffer and centrifuged at 400xg for 5 minutes at 4°C. For intracellular staining, the same procedure as surface staining was done, but after fixation the cells were washed with 1x Permeabilization Buffer (eBioscience) and stained for 45 minutes. For cytokine staining, T cells were stimulated *ex vivo* for 5 hours in 96-well round-bottom plates with 50ng/ml PMA (Phorbol 12-myristate 13-acetate, Sigma) and 500ng/ml ionomycin (Sigma) in the presence of GolgiStop (BD Biosciences) After stimulation, cells were blocked for 20 minutes, fixed for another 20 minutes, washed with permeabilization buffer and stained for 45 minutes (detailed protocols of the staining in annex). The data was acquired on the flow cytometer BD FACSCantoII (BD Biosciences) and the analysis preformed on the software FlowJo (Tree star).

Table 3 – Fluorescent-antibodies used for staining PBMCs.

Antibody	Clone	Supplier
CD11c PE	3,9	eBioscience
CD123 PE-Cyanine7	6H6	eBioscience
CD14 eFluor® 450	61D3	eBioscience
CD19 APC-eFluor® 780	HIB19	eBioscience
CD19 eFluor® 450	HIB19	eBioscience
CD197 (CCR7) PE	3D12	eBioscience
CD24 PE	eBioSN3(SN3 A5-2H10)	eBioscience
CD25 APC-eFluor® 780	BC96	eBioscience
CD27 PE-Cyanine7	O323	eBioscience
CD3 FITC	SK7	eBioscience
CD31 (PECAM-1) PerCP-eFluor® 710	WM-59	eBioscience
CD38 APC	HIT2	eBioscience
CD4 APC-eFluor® 780	RPA-T4	eBioscience
CD4 eFluor® 450	RPA-T4	eBioscience
CD45RA FITC	HI100	eBioscience
CD45RA PE-Cyanine7	HI100	eBioscience
CD56 (NCAM) APC	MEM188	eBioscience
CD62L (L-Selectin) APC-eFluor® 780	DREG-56	eBioscience
CD8α APC	RPA-T8	eBioscience
CD8α PE-Cyanine7	RPA-T8	eBioscience
CXCR5 PE	IgG 2B	R&D
FOXP3 Alexa Fluor® 647	206D	BioLegend/Imtec
γδTCR FITC	B1.1	eBioscience
HLA-DR APC-eFluor® 780	LN3	eBioscience
IFN gamma eFluor® 450	4S.B3	eBioscience
IgD Brilliant Violet(Pacific Blue)	IA6-2	BD
IgE FITC	Ige21	eBioscience
IgM PerCP/Cy5.5	MHM-88	BioLegend/Imtec
IL-17A FITC	eBio64DEC17	eBioscience
IL-2 PerCP-eFluor® 710	MQ1-17H12	eBioscience
IL-4 PE	8D4-8	eBioscience
IL-7Rα (CD127) PerCP-Cyanine5.5	eBioRDR5	eBioscience

Antibodies are listed with antigen target (all human), fluorochrome label, the hybridoma clone and the supplier.

3.7 Activation of B cells transfected with viral vectors containing different mutations in CARD11

Activation potential of B cells was measured via the expression of CD25 in primary mouse B cells genetically altered to express different *CARD11* mutations in collaboration with Dr. Keisuke Horikawa from the Australian National University. Retroviral vectors were constructed in order to express three different variations of CARD11: wildtype (WT), *unmodulated* (*unm*; L298Q)[81], Mut10 (L232LI) [104] and Mut18 (analogous to the human D1152N). WT and mutated *Card11*, were cloned into pMXs-IRES-GFP vector, transfected into Phoenix ecotropic packing cells and retroviral particles collected, as previously described [104].

B cells from Ig^{HEL} transgenic mice were activated into proliferation with hen egg lysozyme (HEL), *in vivo*, and transduced, *in vitro*, with the retrovirus containing the constructs[104]. The transduced B cells were then stimulated *in vitro* with LPS and expression of CD25 on transfected ($^{GFP+}$) cells was assessed by flow cytometry.

3.8 ELISA

The quantitative measurement of plasma cytokines IL-4 and IL-3 from the both patients, five adult healthy controls (32-49 years old), eight children healthy (3-8 years old) controls and one positive control (male lupus patient with 6 years old) was done using the Human IL-4 Ready-Set-Go! ELISA Kit and the Human IL-13 Ready-Set-Go! ELISA Kit (eBioscience). ELISA plates (provided with the kit) were coated with capture antibody in 1xCoating Buffer and incubated overnight at 4°C. Wells were blocked with Assay Diluent for 1 hour, samples and standards (diluted in Assay Diluent in a 2-fold serial dilution starting with 200pg/mL, for the IL-4 ELISA kit, and starting with 500pg/mL for the IL-13 ELISA kit) were added to the plate and incubated overnight at 4°C. Detection antibody was diluted in Assay Diluent, added to the plate and incubated for 1 hour at room temperature. After incubation Avidin-HRP diluted in Assay Diluent was added to the plate and incubated for 30 minutes. Between each previous step, one step of washing was done. Substrate solution was added to each well and plate incubated for 15 minutes at RT. In the end of the incubation, Stop Solution was added, the results were read using Eon™ Microplate Spectrophotometer in a wavelength of 450nm (BioTek, Winnoski, Vermont, U.S.A) and data analyzed in the Gen5™ 2.0 Data Analysis Software (BioTek). Using the standard's serial dilutions, a

logarithmic standard curve was constructed. The kits' minimal detection level was 2pg/mL for the IL-4 ELISA kit and 4pg/mL for the IL-13 ELISA kit. The samples that fell above these values were considered positive and the samples that fell below these values were considered negative or with undetectable levels.

Reagents and Primers

FACS wash buffer:

Make in 20mM PBS:
100% FCS to a final concentration of 2%
200mM EDTA to a final concentration of 1mM
0.1% NaN3 to a final concentration of 0.01%

Blocking buffer:

Make in 20mM PBS:
100% FCS to a final concentration of 10%
0.1%NaN3 to a final concentration of 0.01%
NMS to a final concentration of 2%

2x 5 hours stimulation buffer:

Make in complete RPMI with 2% human antibody serum:
GolgiStop to a final concentration of 1:250
PMA (100µg/ml) to a final concentration of 50ng/ml
Ionomycin (1µg/ml) to a final concentration of 500ng/ml

Complete RPMI with 2% human antibody serum:

Make in RPMI 1640 + L-glutamine (GIBCO):
100% heat inactivated human antibody serum to a final concentration of 2%
10K/10K Pen/Strep to a final concentration of 1%

LB medium/plates:

Make in 500mL of distilled H_2O:

2.5g of Yeast substrate

5g of Tryptone

5g of NaCl

7,5g Agar-agar (plates)

500µL of 100µg/mL Ampicillin (plates)

5x TBE buffer:

Make in 1L of distilled H_2O:

54g of Tris base

27.5g of Boric acid

20mL of 0.5M EDTA

Table 4 –Primer sequences

Primer	Primer Forward	Primer Reverse
CARD11 (gDNA)	5'-CGGCTGAAGGAGAAGGAGCTG-3'	5'-GCCTGTCCCCAGCATTACATT-3'
CARD11 (cDNA)	5'-TCCGGGTGTGTGAGAAGAACATC-3'	5'-GCGTTCTTTGCTCCCCTGTCTC-3'
qPCR CARD11	5'-TTCCTGTCGGGTTTTGCATTTCC-3'	5'-GCAGGGTTGATATAGCGGCTGAG-3'
B-actin	5'-CTGGGACGACATGGAGAAAA-3'	5'-AAGGAAGGCTGGAAGAGTGC-3'
GAPDH	5'-AGAAGGCTGGGGCTCATTTG-3'	5'-GCATCAGCAGAGGGGGCAGA-3'
HPRT	5'-GTAGCCCTCTGTGTGCTCAAGG-3'	5'-GGCTTATATCCAACACTTCGTGGGG-3'
IL-4	5'-GGGCTGCGACTGTGCTC-3'	5'-TCACAGGACAGGAATTCAAGCCCG-3'

4 Results

4.1 Diagnosis of atypical HIES in a Belgian family with Moroccan ethnicity

The patients of this study are the 3rd (P1; female) and 2nd (P2; male) born children from consanguineous, healthy parents. P1 and P2 have a healthy sister (S) and brother (B). P1 and P2 were included in the study at the age of one and three years old, respectively. P2 suffers from severe and progressive eczema on the face and body, severe itching, recurrent skin bacterial infection caused by *S. aureus*, formation of pustules and abscesses, recurrent respiratory infections by *H. influenza* with persistent rhinitis, congested nose and viral wheezing. Laboratory analysis from P1 and P2 show progressively increased levels of serum IgE. Although patient P1 was the first patient in the studies due to sample availability, her phenotype is less severe that the one of patient P2. Also, while patient P2 is under heavy medication of antibiotics (oral and dermal) and inhaled steroids (to ameliorate the asthma-like phenotype), patient P2 only applies dermic antibiotics to control eczema and sporadic infections. Additionally, clinical laboratory analysis, performed by the hospital's analysis laboratory, of P1 showed an aberrant TNFα response after stimulation with LPS and Zymosan and decreased lymphocytes. P2 also presented decreased levels of lymphocytes, increased $CD8^+$ T cells and higher levels of IgA. Detailed immunological results from the laboratory analysis are listed in Table 5.

Table 5 – Immunological information provided by laboratory analysis from patient 1 and 2.

Parameter	Patient 1 (born in 2010)			Patient 2 (born in 2007)		
	May 2011	**Sept 2011**	**Dec 2011**	**Jan 2010**	**Feb 2010**	**Feb 2013**
Total lymphocytes	-	2100 cells/µL (4000-10500)	-	-	-	1300 cells/µL (2000-8000)
$CD8^+$ cells	-	-	-	2012 cells/µL (300-1600)	-	-
Total IgE	316 IU/L (≤51)	747 IU/L (≤91)	782 IU/L (≤91)	1505 IU/L (≤159)	1688 IU/L (≤159)	3408 IU/L (≤224)
IgA	-	-	-	1.55 g/L (0.23-1.24)	-	-

Discrimination of immune related parameters which values were not between the age-matched upper and lower limits (empty cells mean that the evaluation of the parameter fell in the normal age-matched limits).

4.2 Immunological profile

Immunologic analysis was performed on P2, since this was the oldest patient and the phenotype was more accentuated than in P1. To evaluate the immunologic characteristics of the patient we used flow cytometry analysis on PBMC's of the patient and age-matched controls. From the comparison of patient's immune populations with the norm of the immune populations of the controls, we observed that the percentage of total leukocytes was located at the high end of the normal range (Figure 4A), while NKT cells were at the low end (Figure 4B). Non-B cell, non-T cell and non-monocytes population were decreased by more than one standard deviation (SD) (Figure 4C), and so were natural killer cells (Figure 4D) and both myeloid and plasmacytoid dendritic cells (Figure 4E,F).

Analysis of the lymphocyte population show normal frequencies of total lymphocytes (Figure 5A) and T cells (Figure 5B). In the T cells compartment, $CD4^+$ cells were more than one SD above the norm (Figure 5C), while $CD8^+$ cells (Figure 5D), double negative T (Figure 5E) cells and γδ T cells (Figure 5F) were within the normal range of the controls.

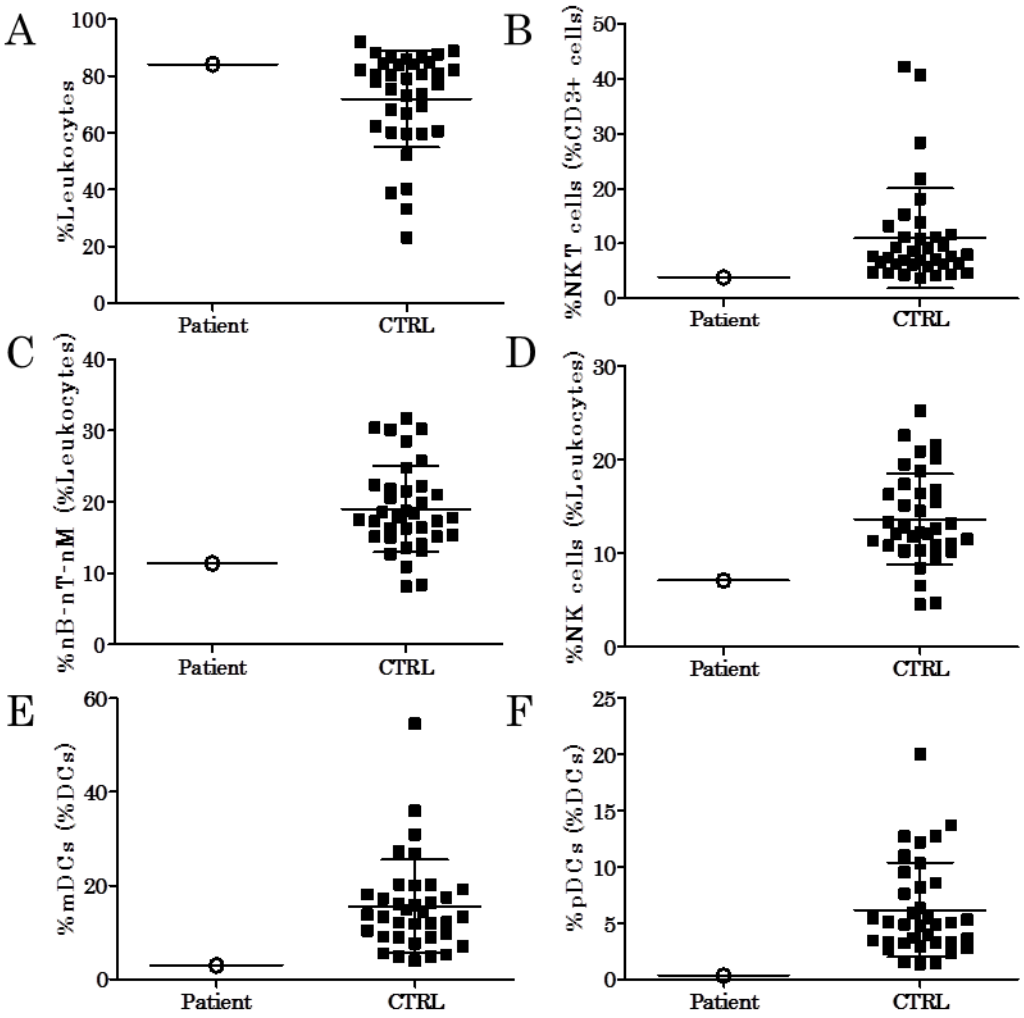

Figure 4 – Most leukocyte subpopulations are altered in HIES patient P2. Flow cytometry data for PBMC for patient P2 and age-matched controls (n=36). In the figure are represented the percentages of **(A)** leukocytes among PMBCs, **(B)** NKT cell amongst CD3+ cells, **(C)** non-B, non-T and non-monocytes cells from the total leukocytes, **(D)** NK cells among leukoytes and **(E)** mDCs and **(G)** pDCs amongst the DC population.

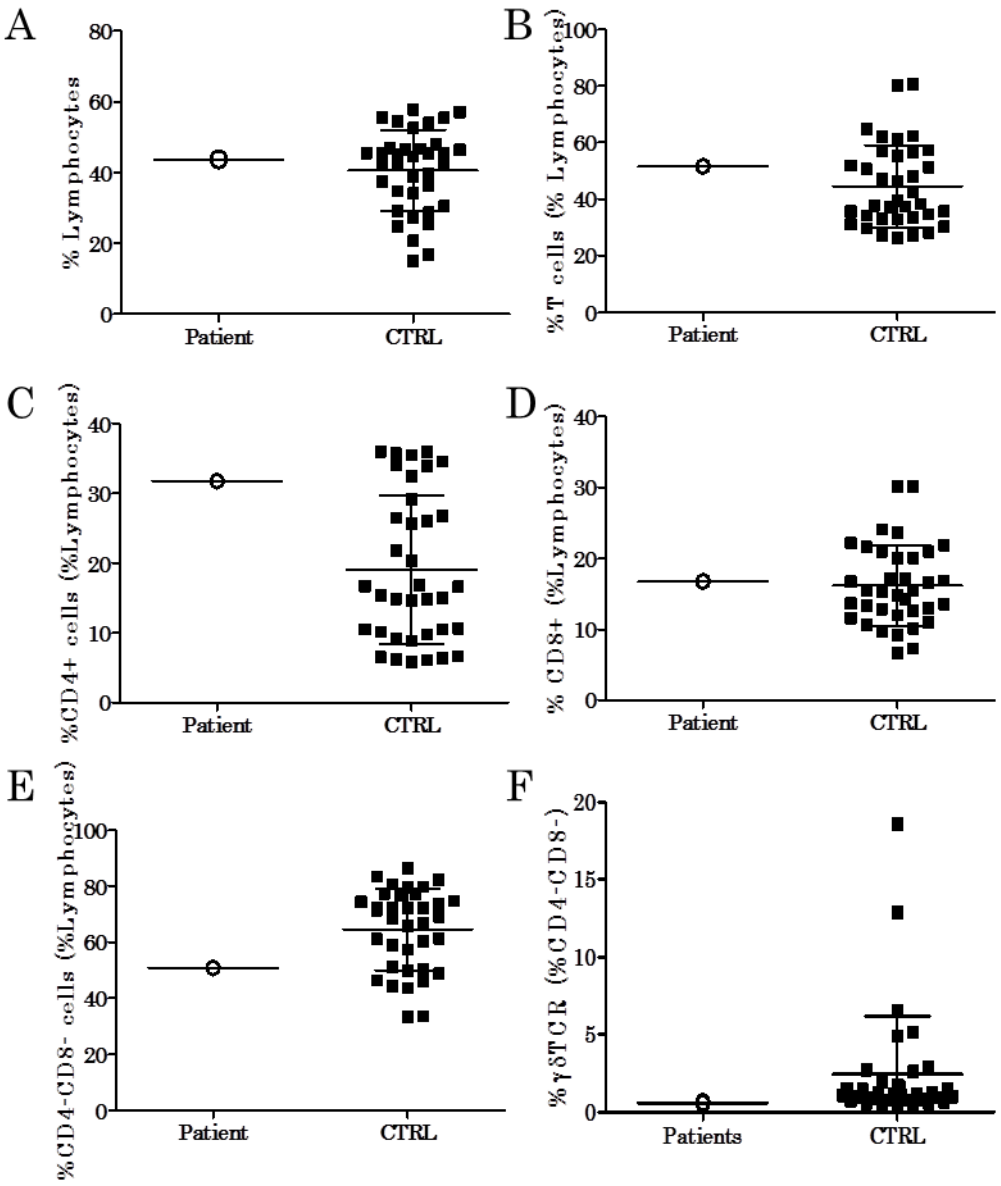

Figure 5 – Alteration in T cell population in HIES patient P2 is limited to an increase in CD4$^+$ T cells. Flow cytometry data for PBMC for patient P2 and age-matched controls (n=36). Percentage of **(A)** lymphocytes among PMBCs, **(B)** T cells among lymphocytes, **(C)** CD4$^+$ T cells among lymphocytes, **(D)** CD8$^+$ T cells among lymphocytes, **(E)** double negative T cells among lymphocytes and **(F)** γδ T cells among lymphocytes.

Within the $CD4^+$ population, the naïve subset was reduced by more than one SD (Figure 6A), with a particular decrease in recent thymic emigrants (RTE) (Figure 6B,C). T_{regs} were sharply reduced with an observed value lower than all control samples (Figure 6D). Among the antigen-experienced T cell subsets, central memory T cells (TCM) were at the high end of the normal range (Figure 6E), effector memory T cells (TEM) were increased by more than one SD (Figure 6F), and $CD45Ra^+$ TEM (TEMRA) were unaffected (Figure 6G). Among $CD8^+$ subpopulation, naïve cells (and RTE) were at the lower end of the normal range (Figure 7A,B), while antigen-experienced cells were greatly increased – TCM by more than 6 SD from the norm (Figure 7C) and TEM by more than 1 SD (Figure 7D). As with CD4 T cells, CD8 TEMRA were unaffected (Figure 7E). Together these results indicate a defect in CD4 T cells production and Treg conversion, and elevated T cell activation, especially in the past (with the central memory population increased to the greatest extent).

Within the effector T cell population, flow cytometry data show a decrease of more than 1 SD in Tfh cells (Figure 8A) and a normal population of IL-2 producing $CD4^+$ T cells (Figure 8B) and Th1 cells (Figure 8C). Interestingly, Th2 cells, which are responsible for the secretion of cytokines that promote IgE production, were decreased by more than one SD (Figure 8D). Th17 cells were also reduced by one SD (Figure 8E). This reduction of Th17 cells in the patient matches what has been described for *STAT3*-derived HIES patients. Among the CD8 population, IFNγ producing cells were reduced by one SD (Figure 8F) and, as in CD4 population, IL-2 producing cells were within the normal rage (Figure 8G).

Concerning the B cell populations, results show normal populations of total B cells (Figure 9A), naïve (Figure 9B), switched (Figure 9C), IgE-producing cells (Figure 9D) and memory B cells (Figure 9E), while immature B cells (Figure 9F) and plasmablasts (Figure 9G) were decreased by more than one SD.

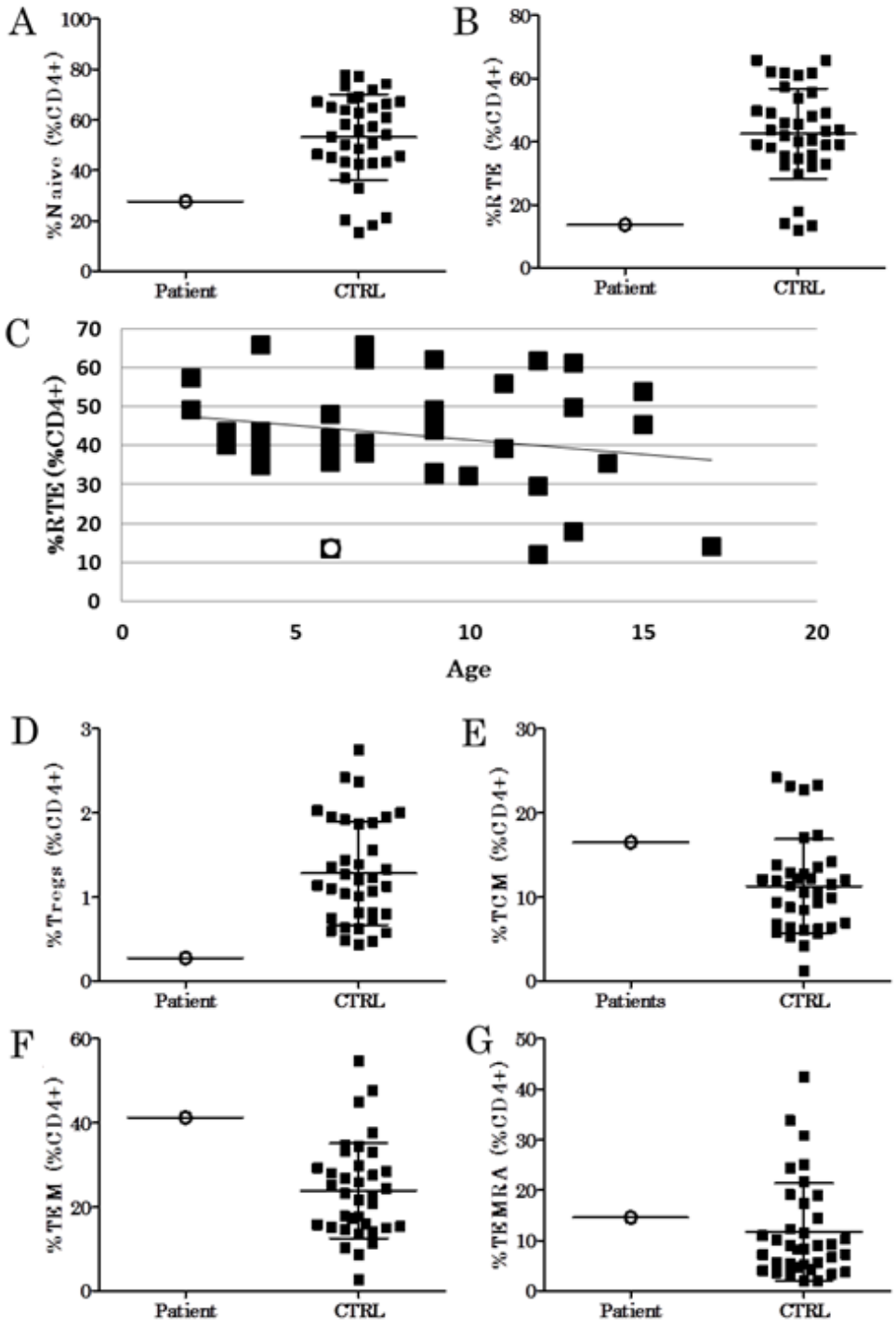

Figure 6 – Alterations in CD4$^+$ T cells affect naïve, memory and Treg subpopulations. Flow cytometry data for PBMC for patient P2 and age-matched controls (n=36). Percentage of **(A)** naïve cells **(B)** recent thymic emigrants, **(C)** Correlation of the frequency of CD4$^+$ recent thymic emigrants with age **(D)** regulatory T cells, **(E)** central memory T cells, **(F)** effector memory T cells and **(G)** CD45$^+$ effector memory T cells among the CD4$^+$ population. (■ = healthy controls; ○ = patient P2)

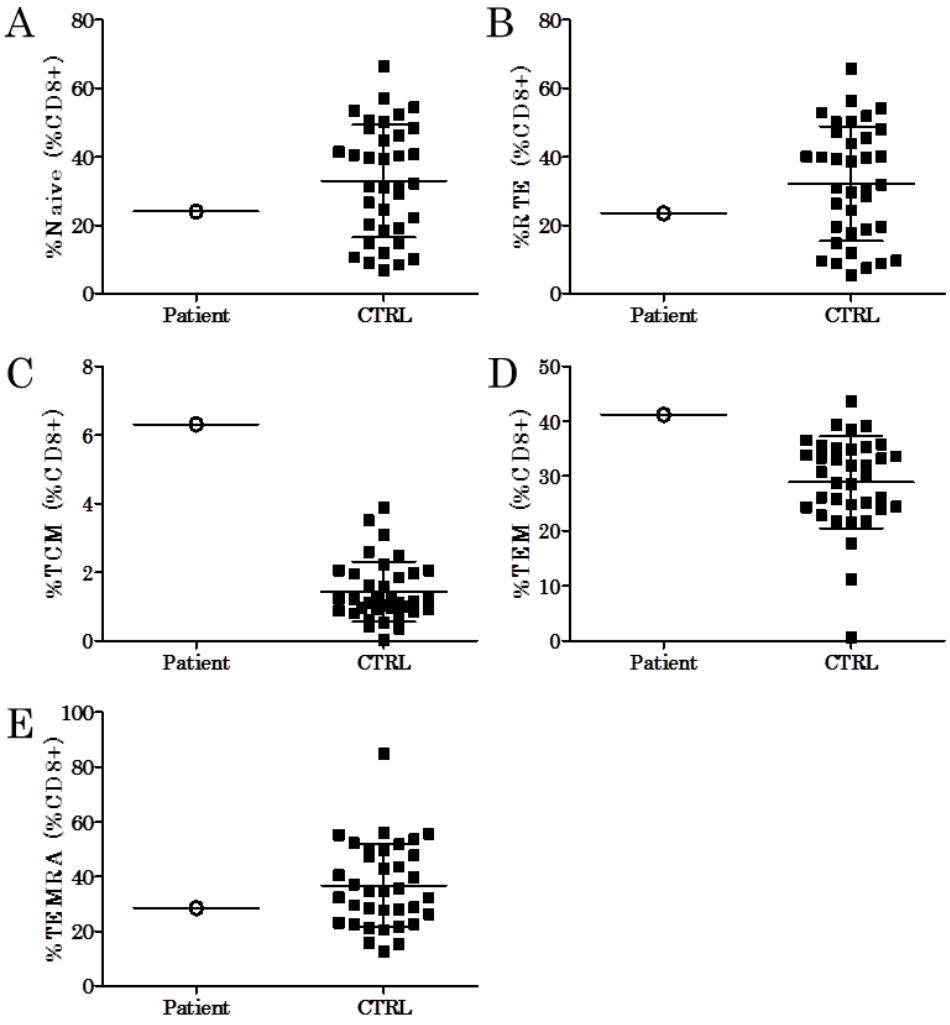

Figure 7 - Variations in CD8$^+$ T cells are found among the memory subpopulations in the HIES patient P2. Flow cytometry data for PBMC for patient P2 and age-matched controls (n=36). Percentage of **(A)** naïve cells **(B)** recent thymic emigrants, **(C)** central memory T cells, **(D)** effector memory T cells and **(E)** CD45$^+$ effector memory T cells among the CD8$^+$ population (■ = healthy controls; ○ = patient P2)

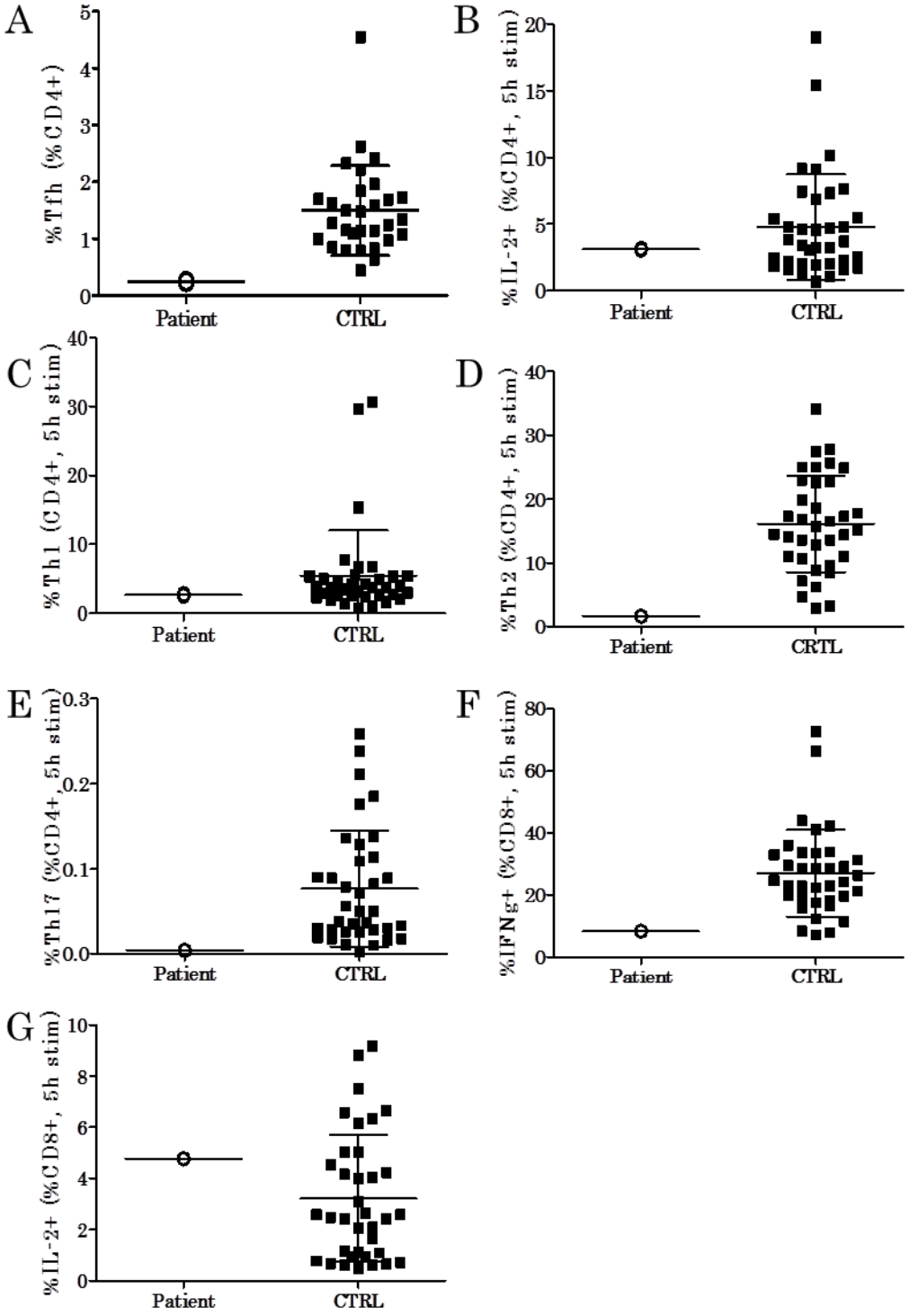

Figure 8 – Helper T cell populations and CD8 cytotoxic T lymphocytes are decreased in the HIES patient P2. Flow cytometry data for PBMC for patient P2 and age-matched controls (n=36) after 5h stimulation with PMA and ionomicyn. Percentage of **(A)** folicular helper T cells, **(B)** interleukin 2-producing cells, **(C)** type 1 helper T cells, **(D)** type 2 helper T cells and **(E)** helper T 17 among the $CD4^+$ T cells. **(F)** cytotoxic T cells and **(G)** interleukin 2-producing cells among the CD8 T cell population.

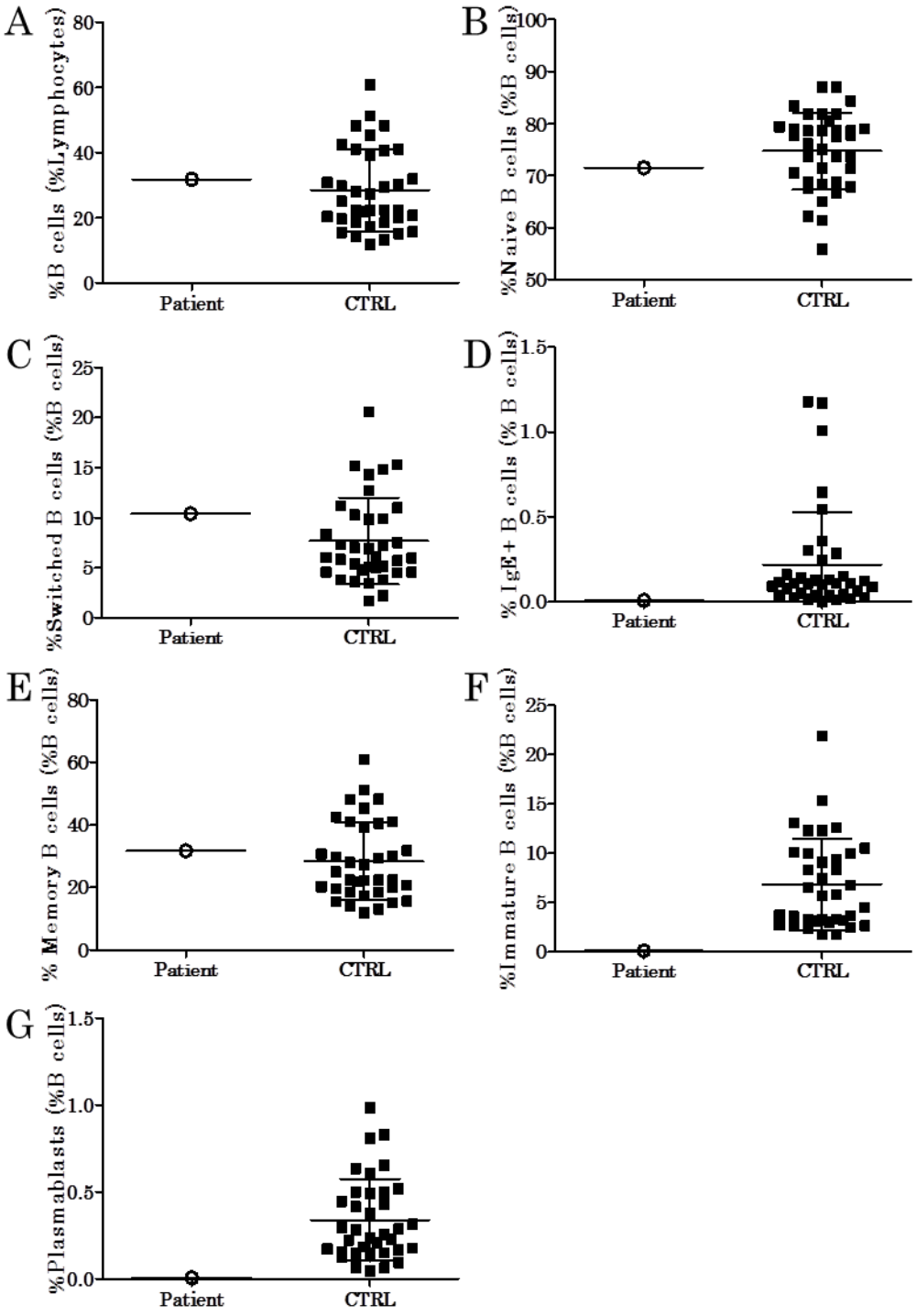

Figure 9 – The B cell compartment of the HIES patient P2 is marked by a decrease in immature B cells and in plasmablasts. Flow cytometry data for PBMC for patient P2 and age-matched controls (n=36). Percentage of **(A)** B cells among lymphocytes, **(B)** naïve cells, **(C)** switched cells, **(D)** IgE-producing**, (E)** memory, **(F)** immature and **(G)** plasmablasts among the B cell population.

4.2.1 Expression and secretion of IL-4 and IL-13 is not increased above healthy levels in patient P1 and P2

Production of IL-4 and IL-13 is the hallmark of a Th2-mediated response and is required to promote IgE secretion. In order to quantify the expression and secretion of IL-4 in the patients, qPCR and ELISA assays were performed. We measured IL-4 mRNA expression in the PBCMs of both sick and healthy members of the patients' family and normalized it to β-actin, GAPDH and HPRT mRNA expression. Results show no increase or decrease of IL-4 expression in the patients compared to the healthy members of the family (Figure 10A). To measure the secretion of IL-4 we ran an ELISA assay on the plasma of the patients against age-matched and adult healthy controls and a systemic lupus erythematosus patient, which we used as a positive control. The results corroborate the normal expression of IL-4, as levels of plasma IL-4 were below detection levels (<2 pg/mL) for both patients and healthy controls and for the positive control IL-4 levels were at 3,12pg/mL (Figure 10B). Additionally, ELISA assay to detect levels of IL-13 was also performed and results are similar to the ELISA for IL-4. Levels of plasma IL-13 were below detection levels in the patients, in all the healthy controls and the patient with lupus (data not shown). These results show that the activity of Th2 cells is not increased.

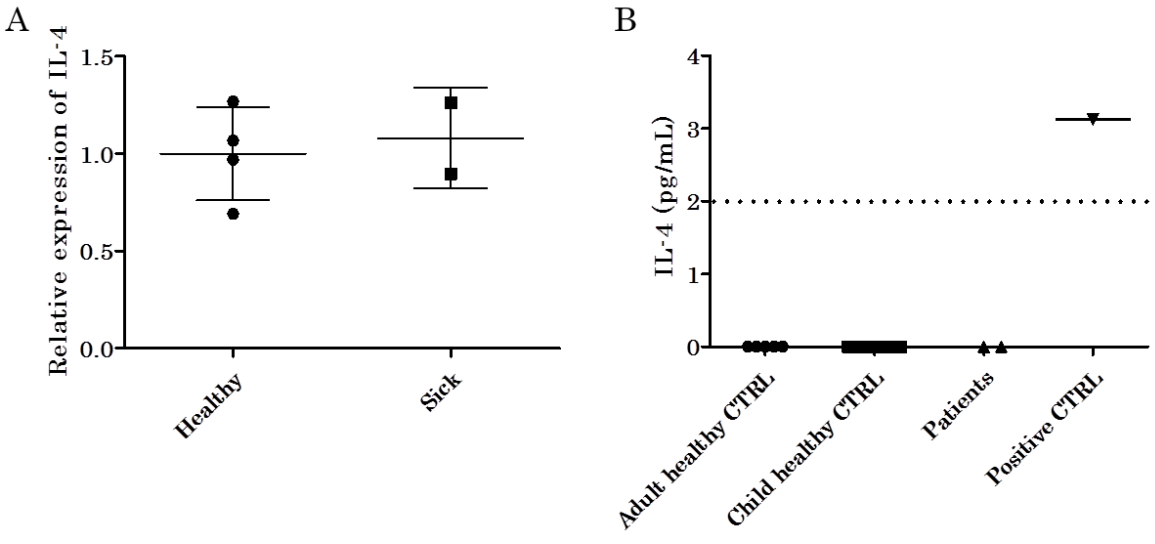

Figure 10 – Levels of expression and secretion of IL-4 are normal in the patients. (A) qPCR and **(B)** ELISA assay show that the expression and secretion levels of IL-4 are neither increased or decreased in patients, compared to the controls. Dash line represents the detection limit of the assay (2 pg/mL).

4.3 CARD11: the candidate gene

Whole exome sequencing (WES) of P1 was performed to search a possible candidate gene to explain the patient's phenotype. The exome analysis was performed only in P1 since she developed the phenotype at a younger age than P2 and blood from P2 was not available at the time. The assumption was made that the disease was caused by Mendelian inheritance, due to the severity and early age of onset, the occurrence of the disease in siblings and Mendelian inheritance of all explained HIES cases. Therefore common polymorphisms were removed from the whole exome sequencing results of P1, by filtering out intronic, synonymous or non-rare variants, i.e. hits with allelic frequency greater that 0.5% in dbSNP, 1000 Genomes, HapMap or YH. The filtering resulted in 1663 identified variants in 1164 genes. 205 genes had more than one mutation, making them potential compound heterozygotes. From the 1164 genes 5 were found to be related to high levels of serum IgE, one of which is a compound heterozygous (Figure 11): *CARD11, CBL, FLG, HLA-DRB1* and *RAD50*. From these 5 genes, we chose a candidate taking in consideration the quality of the whole-exome sequencing read, prediction of alterations on protein function and structure, frequency and phenotypic similarities with previous studies (Table 6). Homozygous variants were also analyzed but none was classified as a suitable candidate.

Mutations in *FLG* are known to cause a primary skin/hair disease, with hyper-IgE only developing as a secondary effect. Additionally, the *FLG* locus was identified as a region of low sequencing quality with multiple variants detected in healthy individuals. The *FLG* mutation is therefore probably a false positive, and as the clinical presentation did not fit, this candidate was discarded. *HLA-DRB1* variants were identified as influencing IgE levels in GWAS. However the HLA locus is the most polymorphic locus in human, with most of the variability as yet undiscovered. Furthermore, the mode of activity of *HLA-DRB1* variation is known, as it alters the presentation of various peptides, resulting in relatively subtle shifts in the efficacy of responses towards infection. *HLA-DRB1* mutations are therefore inconsistent with the biology of HIES. GWAS identified *RAD50* variants as being linked to IgE levels. However, this gene contains a locus control region known to play an important role in regulating Th2 cytokine gene transcription and is also located within the Th2-cytokine locus and that several other candidate genes for atopy-related traits, such as increased IgE levels, have been mapped in this region. Therefore, it is difficult to conclude, from GWAS, whether the increased levels of IgE is a result of variations in *RAD50* or in

other genes from that region. Additionally, studies relating increased levels of IgE have been done in a healthy population, from which IgE levels were available, or in asthmatic patients. Because the phenotype of the subjects of GWAS did not match the phenotype of our patient and the location of the *RAD50* region includes also Th2-cytokine genes, *RAD50* was excluded from the candidate genes. *CBL* has been related to increased levels of IgE in knock-out mice; however this was true only in *SLP-76/Cbl* double knock-out mice. For that reason, *CBL* gene was disqualified as a candidate gene.

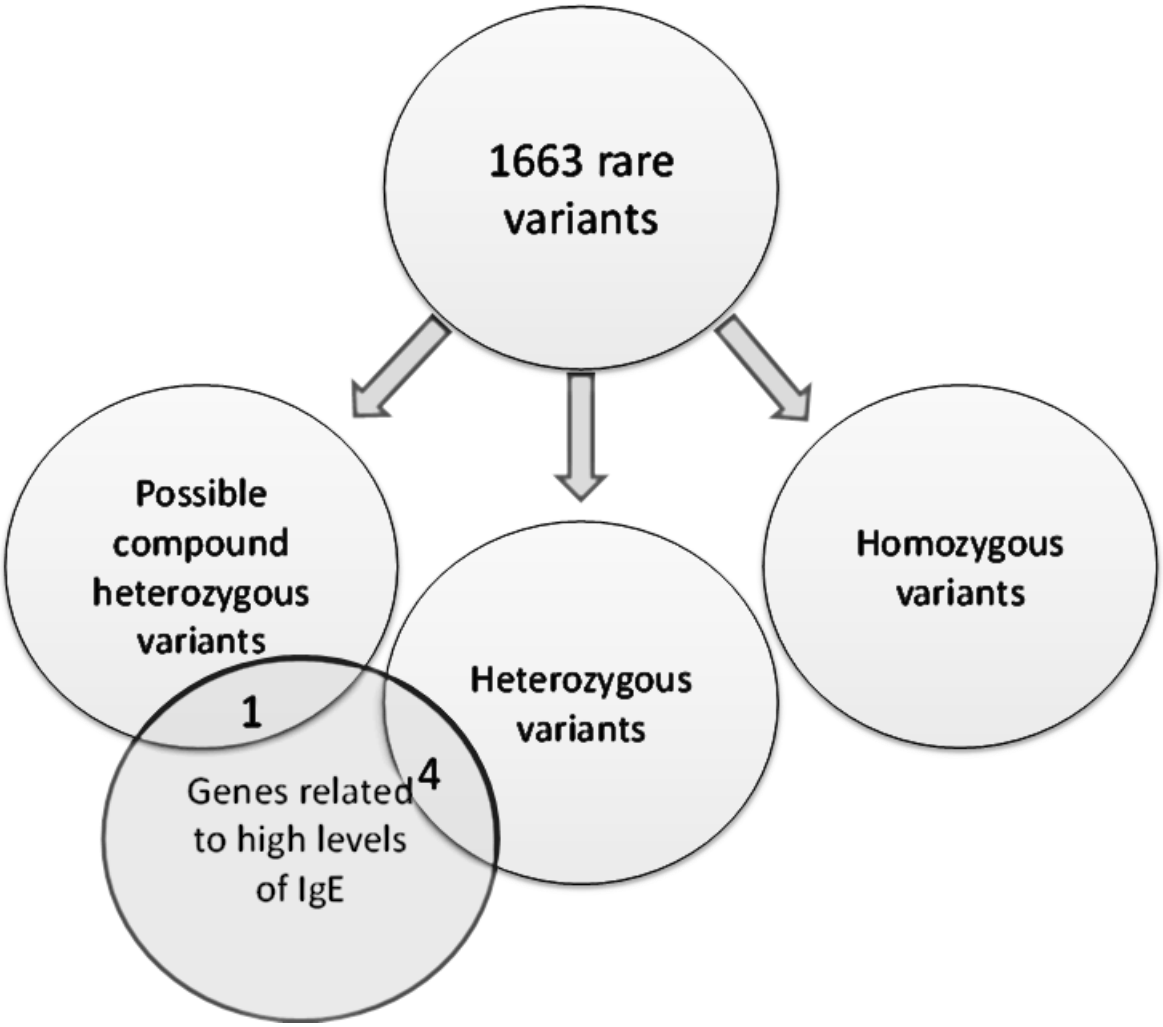

Figure 11 – Overlap of whole exome sequencing (WES) hits with genes related to high levels of-IgE. From the 1663 variation hits form WES we sorted the genes that had a single variation and the genes that had two or more variants. We then crossed these genes with the list of HIES-related genes to find our candidate genes.

We found CARD11 to be the best candidate gene due to multiple factors: i) the sequencing was of high quality with depth of 149 and a read quality of 99, ii) the variation was predicted to be damaging to the protein, iii) the variation is very rare in

internal and public databases (in dbSNP, the variation rs147422861 has Minor Allele Frequency of 0.002%), and iv) a mouse model with a similar phenotype has been described which not only presents with hyper-IgE but is similar to the patients in the development of dermatitis and the reduced number of T_{regs}. The variation is located in the end of the last exon in the 3454 where a cytosine(C) is substituted by a thymine(T) (C3454T) and causes an amino acid change in position 1154 where aspartate (D) is replaced by asparagine(N) (D1154N). This variation in located in the end of the GUK domain of CARD11.

Table 6 – Characterization of candidate genes.

Gene	# of mutations	Type of mutation	Quality of the read[1]	Polyphen-2 prediction	SIFT prediction	Prediction from Spliceman[2]	Frequency in internal database[3]	Previous studies
CARD11	1	Missense	Good	Possibly Damaging	Damaging	-	Unique	Mice with: Skin condition; Hyper-IgE; Treg deficiency
CBL	1	Splice site	Good	-	-	61% likely the mutation is to disrupt splicing	Unique	CBL/SLP-75 double KO mice: Hyper-IgE
FLG	5	Missense	Poor	Benign	Tolerated	-	Frequent	Mice with: Skin condition; Hyper-IgE
				Possibly Damaging	Tolerated	-		
				Benign	Tolerated	-		
				Benign	Tolerated	-		
			Good	Benign	Tolerated	-	Unique	
HLA-DRB1	1	Missense	Good	Possibly Damaging	Damaging	-	Frequent	Genome wide association study
RAD50	1	Missense	Good	Possibly Damaging	Damaging	-	Unique	Genome wide association study

[1] Read was considered good when for a heterozygous mutation allele ratio was around 50:50 and poor when it skewed more than 10% from the 50:50 ratio.

[2] http://fairbrother.biomed.brown.edu/spliceman/index.cgi

[3] Variants that were found once in the database are classified as unique, variants that were found less than 5 times are classified as rare and variant found more than 5 times are considered frequent

4.4 rs147422861 is present in both patients and two healthy relatives

Following the identification of the *CARD11* SNP rs147422861 we genotyped the family and 370 healthy controls for the *CARD11* SNP by Sequenom. The results indicate that patient P1, patient P2 and the father (F) are heterozygous for the SNP, whereas the mother (M) and the healthy sister (S) are homozygous for the normal allele. The identification of the same SNP in patient P2 was suggestive of a role in the disease.

Results of the Sequenom on the brother (B) were not satisfactory, therefore the genotype was confirmed by Sanger sequencing. The sequencing revealed that the brother was heterozygous for the SNP (Figure 12A). These results show a low incidence of the SNP in population, where from 376 analyzed samples only 4 were found to possess the variation. While, constructing the family tree and genotyping each member we observed that rs147422861 was passed from the father to the patients and the healthy brother but not to the healthy sister (Figure 12B). While these results are not consistent with a dominant positive inheritance pattern, we formally checked for a dominant negative activity.

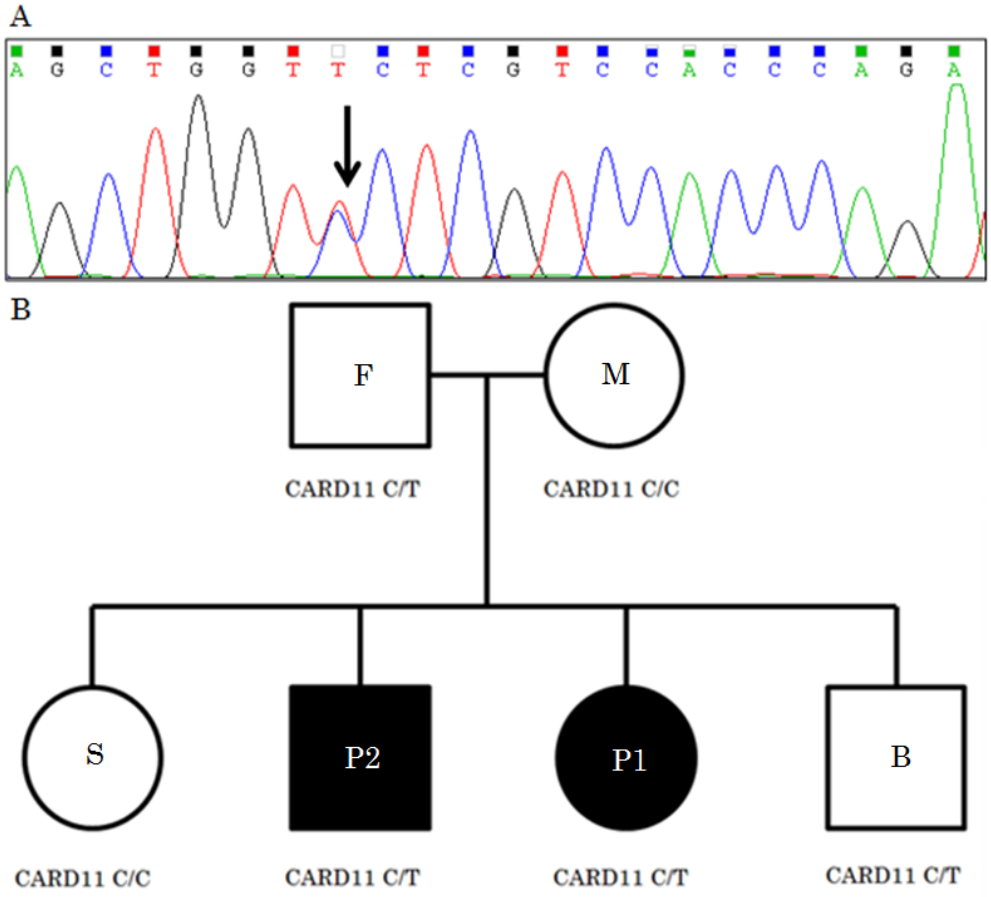

Figure 12 – Inheritance of the *CARD11* variant. (A) CARD11 genotype confirmation of sample B. Genotyping results for the SNP rs147422861 by Sanger sequencing show that B is heterozygous. Black arrow indicates the site of the mutation. **(B)** Schematic representation of the direct family of the patients with corresponding genotype for CARD11. Squares represent males, circles represent females, white symbols represent healthy individuals and black symbols represent individuals with HIES. Progeny is displayed from the oldest to the youngest (left to right).

4.5 Mutation D1154N (mut18) does not affect the expression of CD25 in murine B cells

In mice, mutations in *Card11* that cause HIES are hypomorphic in nature. Therefore, to generate a dominant inheritance pattern, the D1154N mutation in *CARD11* would have to have a dominant negative function. To test this hypothesis, we studied the effects that mutations in *CARD11* might have in B cell activation, testing several variations of the gene, separately or together. We generated three retroviral vectors to carry one or two of the three variations. The variations were two known mutations, one dominant positive (mut10) and one dominant negative (*unm*), and one with the mouse analogue of the D1154N CARD11 mutation (mut18). Transformed mouse B cells were stimulated *in vitro* with LPS, which promotes the activation of B cells and thus expression of CD25. The vector containing the mutated or normal gene also expressed green fluorescent protein (GFP), and therefore transformed B cells were identified using the fluorescent protein. Expression of CD25 was measured on transformed cells expressing GFP by flowcytometry (Figure 13A).

Data show that B cells transformed with CARD11 mut10 had a higher expression of CD25 than the WT, confirming the dominant positive effect of the mutation. When this mutation was expressed together with the unmodulated (unm) expression of CD25 as normalized, confirming the dominant negative effect of the unm mutation. However, when mut10 and mut18 are expressed together, CD25 expression stayed at the same levels as mut10 alone, suggesting that this last mutation does not have a dominant positive or negative effect in the activation of B cells and expression of CD25 (Figure 13B). Together these results corroborate a non-dominant inheritance of the SNP.

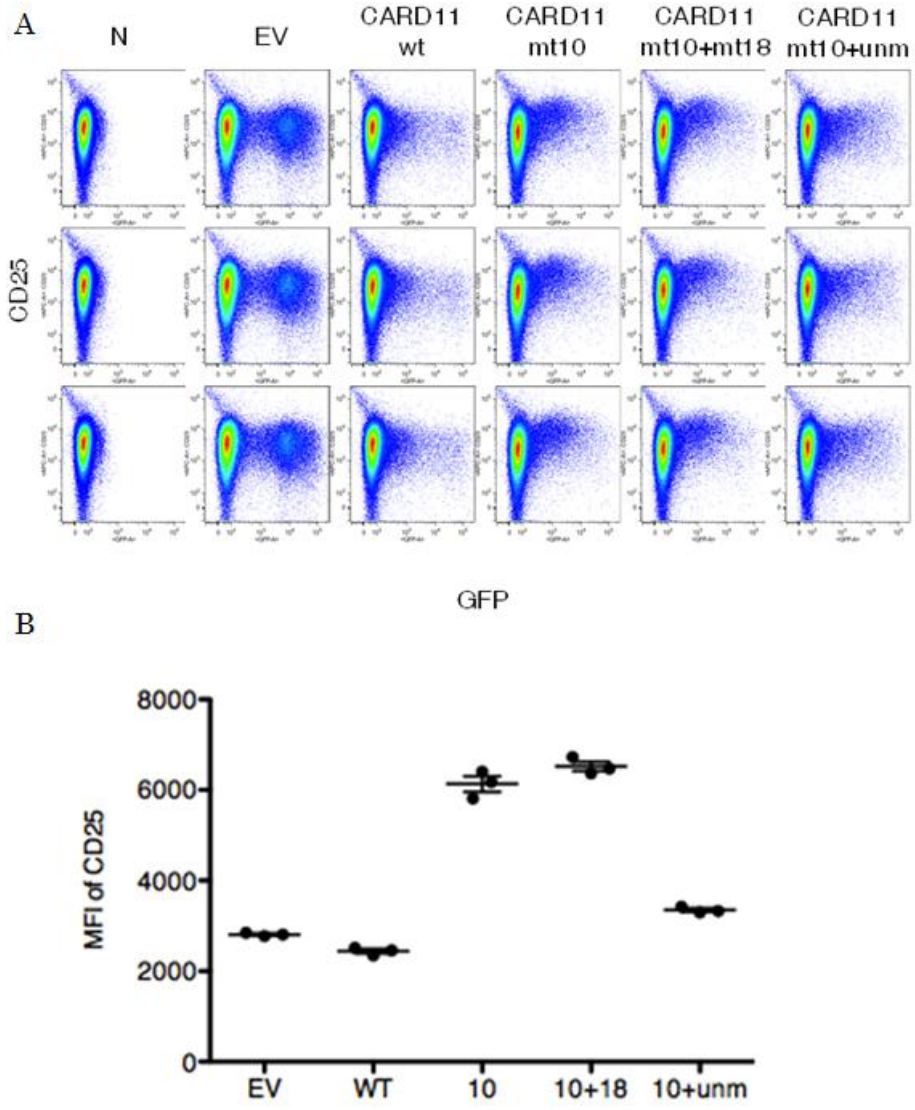

Figure 13 – No dominant negative function of the D1154N CARD11 mutation. (A) Transformed B cell population expressing CD25. **(B)** Medium fluorescence intensity (MFI) of CD25 in each B cell population expressing the mutations. Expression of CARD11 mut10 increases the levels of CD25 and expression of CARD11 mut10+unm restores CD25 expression to WT levels. Levels of CD25 remains at levels observed when CARD11 mut is expressed when CARD11 mut18 is expressed with CARD11 mut10.

4.6 CARD11 expression is not altered

As the *CARD11* heterozygous SNP was highest quality candidate, yet dominant inheritance was excluded (section 4.5), we therefore tested the possibility that a non-exonic SNP in *CARD11* was cosegregating in the family, creating compound heterozygotes in patient P1 and P2, while leaving carriers unaffected. To do so, we first aimed to look for differences in *CARD11* expression between the family members,

discriminating the healthy from the sick, the parents, sibling and patients, and the carriers of the mutation from the non-carriers, we measured the gene expression in PBMCs by qPCR and the relative expression was normalized to the average of *β-actin*, *GAPDH* and *HPRT*. We saw that between carriers and non-carriers (Figure 14C) and siblings and patients (Figure 14B) *CARD11* is equally expressed. When we compared siblings and patients with the parents a slight, but not significant, increase in the relative expression of *CARD11* was observed (Figure 14B). Also, when relative expression was compared between the healthy and sick family members, a slight but non-significant decrease was observed in the sick individuals (Figure 14A). These results suggest that expression in *CARD11* is not altered in the patients when compared to the healthy controls nor it is altered when comparing mutation carriers with non-carriers.

After confirming that CARD11 expression did not vary significantly, we wanted to test if a non-exonic variant was affecting the expression of the normal allele and leaving only the mutant allele to be expressed. In order to determine whether an unobserved mutation was affecting the expression of one copy of *CARD11*, we sought to determine if the D1154N and unmutated alleles were expressed in the same proportion. To accomplish this, an allele-specific expression assay was developed and performed (Figure 14D). gDNA from patient P2 was used as an internal control where 50% of the colonies should carry one allele and the other 50% the second allele. cDNA from the mother (M) was used as a homozygous control to confirm the assay was working effectively. cDNA from patient P1 and P2, brother (B) and father (F) were analyzed. As expected, the percentage of colonies carrying both alleles from the gDNA of patient P2 was approximately 50:50 and the percentage of colonies carrying the common allele from the mother's sample was 99%. Similarly to the genomic control, cDNA from all the heterozygous individuals (P1, P2, F and B) showed a 50:50 ratio of colonies expressing each allele or a preponderance of wild-type expression. None of the heterozygous individuals showed a skewing towards the D154N allele, excluding the possibility of a non-exoninc expression-altering allele on the other copy of *CARD11* These results eliminate the possibility of a simple recessive inheritance of HIES due to *CARD11* mutation in this family

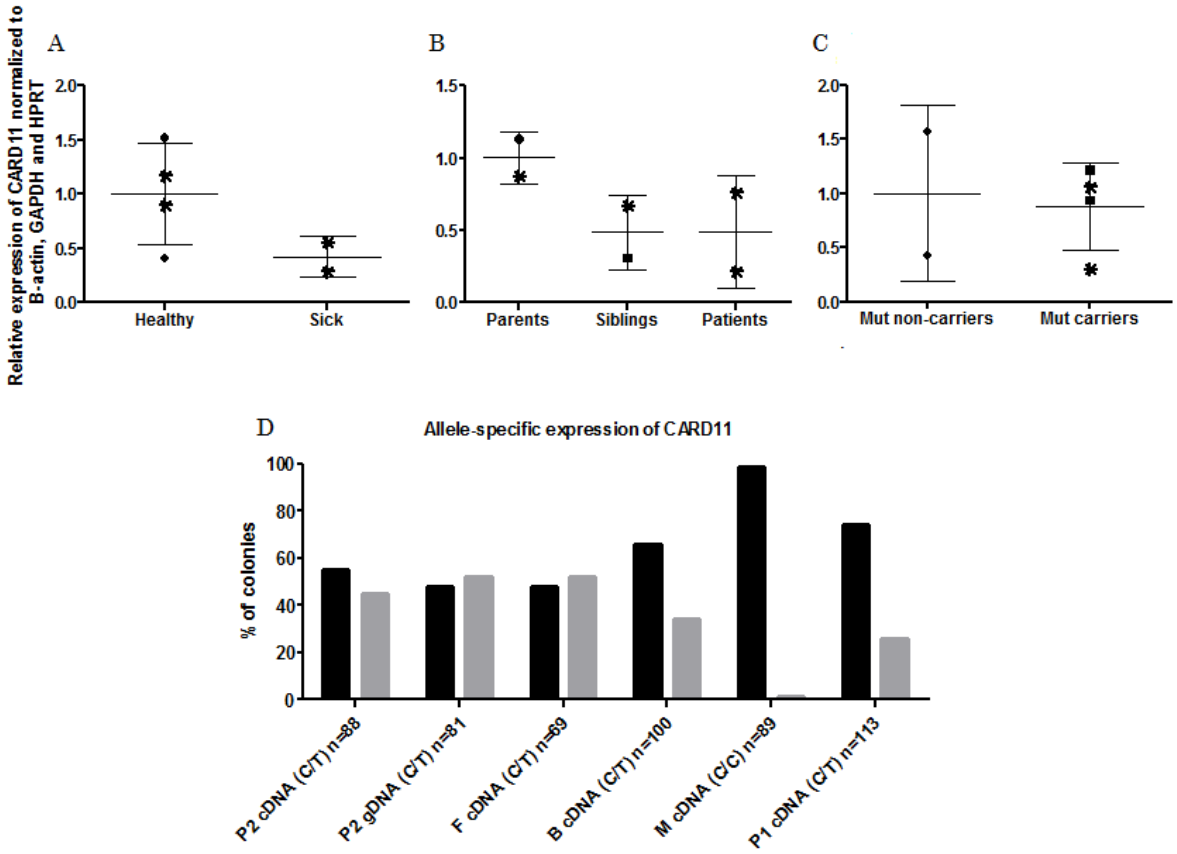

Figure 14 – Relative expression and allele-specific expression of CARD11 are at normal levels. No difference is observed in the expression of CARD11 between **(A)** healthy and sick individuals, **(B)** parents, patients and siblings, and **(C)** carriers and non-carriers of the mutation. **(D)** Allele-specific expression of CARD11 show that either the common is more expressed than the rare allele or that they are expressed in the same proportion (the black bars represent the percentage of colonies expressing the wild-type allele and the grey bars represent the percentage of colonies expressing the rare SNP) .
(*) represents the carriers of the mutation in (A) and (B), and the patients in (C).

5 Discussion

Hyper-IgE syndrome is clinically characterized by recurrent skin and airway infection and greatly increased levels of serum IgE. The most common pathogens in this skin and respiratory infections are *S. aureus* and *H. influenza*, respectively. This is observed in both forms of HIES and also in the patients in this study, placing them in the HIES category. Typical HIES patients manifest not only immunological features but also systemic. In all classic forms of HIES, the increased levels of IgE originate from an enhancement in Th2 differentiation and consequent IL-4 and IL-13 production [51,66,72]. In normal conditions Th2 cells are tightly regulated by the production of IL-10 by T_{regs} and production of the cytokines IL-12 and IFNγ by Th1 cells. In *STAT3*- and *TYK2*-related HIES the formation and activation of T_{regs} and Th1 cells is impaired and the regulation these cells normally exert on Th2 cells is weakened [53,75]. In this study patient P2 presents a normal population of Th1 cells, slightly low T_{regs} and, unexpectedly, reduced Th2 population and lower expression of IL-4 and IL-13 (Figure 10). This reduction in Th2 cells could not be explained by the medication of the patient. The treatment includes inhaled corticosteroids to treat the respiratory symptoms; however there is no indication that this treatment affects Th2 cells. Interestingly, IgE-expressing B cells remain at normal levels, this may be because memory B cells, which are the ones that express surface IgE cells are located in the lymph nodes, which means circulating IgE-positive cells remain low in the periphery.

Defects in Th17 cells are often observed in HIES patients and explains the susceptibility to bacterial and fungal infections [51,69]. We observed in this study that Th17 cells are essentially absent. However, the normal range is also very low and thus the absence of Th17 cells in the patients does not necessarily indicate a major defect and might not be sufficient to account for the recurrent *S. aureus* infections in the patient. Interestingly, it has been reported that *Card11* knock-out mice have a deficiency in the differentiation of Th17 cells [91]. The absence of Th17 cells in the patient could have been explained by the mutation in the patient's *CARD11* if its expression was affected. Other variation in T cell populations have been reported in HIES, such as decreased memory T cells, in both AD- and AR-HIES [51,68], and increased TEMRA cells in the $CD8^+$ population of AR-HIES patients [66]. Our patient does not exhibit such occurrences. In fact we recorded an increase in the TCM cell population and TEM cell population, and normal levels of TEMRA cells. We verified that in the $CD4^+$ population TEM cells are also increased, while TEMRA and TCM remain at normal frequencies. Also, in

unmodulated Card11 mice normal frequencies of effector memory T cells are observed with relative defect in T cell activation or effector/memory cell persistence [83]. In a study of Krampera *et al.*(1999), where the authors report a case of a patient with high serum levels of IgE but with no symptomatology, they found CD8 and CD4 populations diminished and most of the cells were naïve and memory cells, respectively [105]. In our patient the CD4 population was elevated but, as in Krampera study, most of the $CD4^+$ cells were memory cells. Additionally, naïve and RTE $CD4^+$ cells were low, suggesting a decreased thymic output in the patient, which might explain the increased susceptibility to infections, or it can be the consequence of the vast array of infections, since they are known to cause thymic involution leading to a decrease in naïve T cell production. Regarding the CD8 population, it was found to be at normal levels but most of the cells also had a memory phenotype. This results suggest that the IL21R/STAT3 signaling pathway is not impaired, since it has been shown that loss-of-function mutations in *IL-21R* or *STAT3* cause an impairment in the differentiation of $CD8^+$ T cells into memory and effector cells [106].

In AR-HIES, the immune deficiency is commonly characterized with reductions in the total number of lymphocytes, $CD4^+$, $CD8^+$, NK and B cells [55,65–68]. Such reductions did not occur in our patient. The patient had no decrease in the populations of total lymphocyte, $CD4^+$ T cells, $CD8^+$ T cells and B cells, and so *DOCK8* and *TYK2* are implausible candidate genes (even prior to the sequencing data which found no mutation in these genes) although it is noteworthy that NK cells were reduced. The number of total lymphocytes increased in both controls and patient after stimulation. $CD8^+$ cells decreased in both groups and $CD4^+$ cells increased in the control group and decreased in the patient. This might suggest that in the patient although the frequency of $CD4^+$ population is normal, its capability to activate and proliferate in response to stimulation may be affected. In *DOCK8*-deficient patients both CD4 and CD8 populations show a reduced capability of proliferation [69].

Decreased levels and reduced activity of circulating memory Tfh have been observed in patients with deficiency in STAT3 [107]. In our patient the frequency of this population is within normal ranges, though the circulating naïve Tfh population is decreased. Together, these results indicate that the patients described here have atypical immunological presentations, inconsistent with the normal features of *STAT3, DOCK8* or *TYK2*-dependent HIES. Together with the absence of mutations in these genes, this suggests that this family has a novel genetic basis for HIES.

Each form of HIES is characterized by its own collection of systemic features, which are probably related to non-immunological functions of STAT3 and DOCK8. Mutations in both *STAT3* and *DOCK8* have been reported as having non-immunologic consequences; however the same has not been described for TYK2 mutation. The absence of systemic affectations in the patients of this study suggests that the cause for their condition is confined to genes with functions limited to the immune system.

We hypothesized that this disease follows a Mendelian autosomal recessive inheritance due to various observations that point in that direction: i) the patients were born from consanguineous parents; ii) the parents are healthy; iii) the severe phenotype exhibited by the patients and; iv) the commonly observed Mendelian inheritance on HIES.

After categorizing the patient's disease as a novel form of AR-HIES, we sought to find the genetic cause of the patient phenotype. We sequenced the exome of patient P1 and found it to be heterozygous for a rare SNP in *CARD11*. We then investigated the distribution of the SNP in the family. The SNP was passed from the father to both patients and the brother. Given the importance of phenotypic results of mutations in *CARD11* and the presence of a rare *CARD11* SNP in the two patients we selected this gene as the primary candidate. Alterations in the expression of *CARD11/card11* are known to cause immunologic phenotypes in humans and mice. In mice, the overexpression and the knocked down expression of CARD11 causes a HIES-like phenotype. The phenotype of patient P2 is similar to the one in mice with the increased level of serum IgE, the atopic dermatitis, the reduced number of T_{regs}, air-way inflammation and the absence of systemic disorders. However, in mice is observed a Th2-driven immunologic response, an event that in the patient does not occur. This is shown by the reduced frequency of Th2 cells in the patient compared to the age matched controls and by the non-detection of the Th2 cytokines, IL-4 and IL-13.

In humans, *CARD11* mutations have been linked to severe combined immunodeficiency (SCID). A report case by Stepensky *et al.* (2013) characterizes the immunologic profile of a human patient with a 1377bp deletion in CARD11 and reports a reduction in the percentage of T_{regs}, TCM, TEM and TEMRA cells of the $CD8^+$ population, and naïve, switched and memory B cells. They also report an increase in frequencies of γδ T cells and transitional B cells [92]. A second study reveals one more patient with SCID, with predominant naïve phenotype in $CD4^+$ and $CD8^+$ T cells and absent T_{regs} [93]. Most B cells were naïve with a transitional phenotype [93]. Whole-exome

sequencing of this patient revealed it to be homozygous for a SNP in *CARD11*, which introduces a premature stopping codon. Although expressed at the same level of the wild-type form of the gene, the mutation causes a loss of function and a consequent defect in TCR-mediated T cells function due to the non-activation of NF-κB [93]. On the other hand, two gain-of-function mutations in *CARD11* have been related to congenital lymphoid hyperplasia driven by polyclonal accumulation of B lymphocytes [108]. Although these mutations induce the constitutive activation of NF-κB in B cells and in T cells, T cells show a less responsive phenotype when under stimulation [108].

Mutations in *CARD11* have also been described as the cause for diffuse large B cell lymphoma (DLBCL). DLBCL cases can be classified as germinal center B cell-like DLBCL, activated B cell-like (ABC) DLBCL and primary mediastinal B cell lymphoma [109]. ABC DLBCL is characterized by the constitutive activation of NF-κB pathway, which plays a key role in proliferation, differentiation and survival[109]. NF-κB activity is fundamental for ABC DLBCL survival and its inhibition by small hairpin RNA targeting *CARD11* is toxic for the ABC DLBC[110]. The inhibition of CARD11 in ABC DLBCL cells inhibits IKK, which result in the reduced expression of NF-κB target genes [110]. Lymphoma-derived *CARD11* mutations can also induce T cell-independent B cell proliferation, plasmablasts differentiation and auto-antibody production upon chronic binding of self-antigen [104]. Together these results show a conservation of function of CARD11/Card11 between humans and mice, with null function leading to a SCID phenotype in both and a gain of function leading to oncogenic transformation. This conservation of function supported the hypothesis that the HIES phenotype caused in mice by hypomorphic (but non-null) mutations in *Card11* could also be replicated in humans carrying hypomorphic *CARD11* mutations.

Due to the supporting biological basis of *CARD11* mutation causing HIES we further investigated the *CARD11* SNP in the HIES family under investigation. The SNP was passed from the father to both patients and the healthy brother. This observation is not in accordance with a dominant inheritance pattern and the functional assay tested in mice cells carrying the homologous mutations of the patients showed no effect in the activation of B cells. This proves that the mutation does not have a dominant negative activity and consequently the disease is not AD-HIES.

We then hypothesized that the HIES was caused in a recessive fashion, with an exonic mutation inherited from the father and a non-exonic mutation altering expression inherited from the mother. Such an inheritance pattern would allow the father and

healthy brother to be carriers of the non-exonic mutation while remaining healthy due to a wildtype copy. In this scenario, the two patients would need to have inherited both the exonic mutation from the father and the non-exonic mutation from the mother, with the consequence that the only expressed copy of *CARD11* was the mutated hypomorph. To test this, we sought to find differences in the expression of each *CARD11* allele with an allele-specific expression assay. This assay would tell us if a mutation in the promoter of the normal allele could be affecting the expression of that same allele and leaving the carriers of both the mutations (the patients) with only the mutated copy of the gene while the carriers of only the exonic mutation (father and brother) would have a normal expression. Results showed that on both patient P2 and father both alleles contribute 50% each for the total expression of *CARD11*. Although patient P1 and brother had one allele contributing more for the total expression of *CARD11* than the other, the skewing was towards the common allele. This observation rules out the possibility of a mutation in the promoter of the normal allele to be interfering with the balanced expression of the alleles. Together these results rule out *CARD11* as the genetic cause for the patients' phenotype.

6 Conclusions and future work

Several mutations in *CARD11/card11* have been linked to deleterious immunologic features in humans and in mice. In mice, abnormities in the expression of *card11* lead to a HIES-like phenotype, with increased serum levels of IgE, Th2-driven immune response and atopic dermatitis. The patients of this study were diagnosed with HIES, however none of the classical-HIES genes were mutated. The best candidate gene observed was a rare SNP in *CARD11*. Due to the similarities of the patient phenotype to the CARD11-deficient mouse phenotype we wanted to test if, as in mice, *CARD11* was the genetic cause for the phenotype of the patient. Our results ruled out this hypothesis. We did not find any pattern of Mendelian inheritance for *CARD11* and the functional assay in mice showed that this particular mutation does not influence immunologic functions. To further investigate the genetic cause of the patients' disease, whole-exome sequencing or full-genome sequencing of the entire family needs to be performed.

Interestingly, Th2 cells seemed to be decreased compared to the healthy controls. This observation does not correlate to the increased levels of serum IgE, since the increase levels of IgE is Th2-derived. As such other mechanisms of regulation of IgE production may be in action, acting independently and downstream of Th2 signaling or a defect in the binding of IgE to its receptors and consequently increasing its half-life in circulation. Further research will be done in order to clarify the origin of the increased levels of IgE in the patients. The main shifts in T cells populations were found in the naïve and memory $CD4^+$ T cells, T_{regs} and memory $CD8^+$ T cells. Together these results indicate a defect in CD4 T cells production and Treg conversion, and elevated T cell activation, especially in the past (with the central memory population increased to the greatest extent).These observations lead to the tantalizing possibility that HIES in this family is not only novel in terms of the genetic basis, but also in terms of the immunological basis. Further work to identify the disease causation in this family may therefore prove rich in furthering the understanding of IgE production and IgE-mediated disease.

7 References

(1) Ikuta, K., Uchida, N., Friedman, J., and Weissman, I. L. (1992) Lymphocyte development from stem cells. *Annual review of immunology 10*, 795–783.

(2) Janeway, C. a, and Medzhitov, R. (2002) Innate immune recognition. *Annual review of immunology 20*, 197–216.

(3) Moreira, L. O., and Zamboni, D. S. (2012) NOD1 and NOD2 Signaling in Infection and Inflammation. *Frontiers in immunology 3*, 328.

(4) Takeda, K., Kaisho, T., and Akira, S. (2003) Toll-like receptors. *Annual review of immunology 21*, 335–376.

(5) West, a P., Koblansky, A. A., and Ghosh, S. (2006) Recognition and signaling by toll-like receptors. *Annual review of cell and developmental biology 22*, 409–437.

(6) Medzhitov, R., and Janeway, C. (1998) Innate immune recognition and control of adaptive immune responses. *Seminars in immunology 10*, 351–353.

(7) Goldsby, R. A., Kindt, T. J., and Osborne, B. A. (2000) Kuby Immunology 4th ed., p 670. W H Freeman & Co (Sd), New York.

(8) Potaczek, D. P., and Kabesch, M. (2012) Current concepts of IgE regulation and impact of genetic determinants. *Clinical and experimental allergy 42*, 852–871.

(9) Geha, R. S., Jabara, H. H., and Brodeur, S. R. (2003) The regulation of immunoglobulin E class-switch recombination. *Nature Reviews Immunology 3*, 721–732.

(10) Kinoshita, K., and Honjo, T. (2001) Linking class-switch recombination with somatic hypermutation. *Nature reviews molecular cell biology 2*, 493–503.

(11) Xu, Z., Zan, H., Pone, E. J., Mai, T., and Casali, P. (2012) Immunoglobulin class-switch DNA recombination: induction, targeting and beyond. *Nature reviews. Immunology 12*, 517–531.

(12) Murphy, K. (2012) Janeway's Immunology 8th Editio. Garland Science, Taylor & Francis Group, LLC, London and New York.

(13) Hellman, L. (2007) Regulation of IgE homeostasis, and the identification of potential targets for therapeutic intervention. *Biomedicine pharmacotherapy Biomedecine pharmacotherapie 61*, 34–49.

(14) Gonzalez-rey, E., Chorny, A., and Delgado, M. (2007) Regulation of immune tolerance by anti-inflammatory neuropeptides. *Nature Reviews Immunology 7*, 52–63.

(15) Ishizaka, K., Ishizaka, T., and Hornbrook, M. M. (1966) Physico-Chemical Properties of Human Reaginic Antibody: IV . Presence of a Unique Immunoglobulin as a Carrier of Reaginic Activity. *The Journal of Immunology 97*, 75–85.

(16) Gould, H. J., Sutton, B. J., Beavil, A. J., Beavil, R. L., McCloskey, N., Coker, H. a, Fear, D., and Smurthwaite, L. (2003) The biology of IGE and the basis of allergic disease. *Annual review of immunology 21*, 579–628.

(17) Gould, H. J., and Sutton, B. J. (2008) IgE in allergy and asthma today. *Nature reviews. Immunology 8*, 205–217.

(18) Inführ, D., Crameri, R., Lamers, R., and Achatz, G. (2005) Molecular and cellular targets of anti-IgE antibodies. *Allergy 60*, 977–85.

(19) Bestagno, M., Vangelista, L., Mandiola, P. a, Mukherjee, S., Sepúlveda, J., and Burrone, O. R. (2001) Membrane immunoglobulins are stabilized by interchain disulfide bonds occurring within the extracellular membrane-proximal domain. *Biochemistry 40*, 10686–10692.

(20) Achatz, G., Lamers, M., and Crameri, R. (2008) Membrane Bound IgE: The Key Receptor to Restrict High IgE Levels. *The Open Immunology Journal 1*, 25–32.

(21) Batista, F. D., Efremov, D. G., Tkach, T., and Burrone, O. R. (1995) Characterization and expression of alternatively spliced IgE heavy chain trabscripts produced by peripheral blood lymphocytes. *Nucleic acids research 154*, 209–218.

(22) Batista, F. D., Efremov, D. G., Tkach, T., and Burrone, O. R. (1995) Characterization of the human immunoglobulin epsilon mRNAs and their polyadenylation sites. *Nucleic acids research 23*, 4805–4811.

(23) Jensen-Jarolin, E., Achatz, G., Turner, M. C., Karagiannis, S., Legrand, F., Capron, M., Penichet, L., Rodriguez, J. A., Siccardi, A. G., Vangelista, L., Riemer, A. B., and Gould, H. (2008) AllergoOncology: the role of IgE-mediated allergy in cancer. *Allergy 63*, 1255–1266.

(24) Untersmayr, E., Bises, G., Starkl, P., Bevins, C. L., Scheiner, O., Boltz-Nitulescu, G., Wrba, F., and Jensen-Jarolim, E. (2010) The high affinity IgE receptor Fc epsilonRI is expressed by human intestinal epithelial cells. *PloS one 5*, 1–11.

(25) Altin, J., Shen, C., and Liston, A. (2010) Understanding the genetic regulation of IgE production. *Blood Reviews 24*, 163–169.

(26) Deo, S. S., Mistry, K. J., Kakade, A. M., and Niphadkar, P. V. (2010) Role played by Th2 type cytokines in IgE mediated allergy and asthma. *Lung India 27*, 66–71.

(27) Takeda, K., Tanaka, T., Shi, W., Matsumoto, M., Minami, M., Kashiwamura, S., Nakanishi, K., Yoshida, N., Kishimoto, T., and Akira, S. (1996) Essential role of Stat6 in IL-4 signalling. *Nature 380*, 627–630.

(28) Shimoda, K., Van Deursent, J., Sangster, M. Y., Sarawar, S. R., Carson, R. T., Tripp, R. A., Chu, C., Quelle, F. W., Nosaka, T., Vignali, D. A. A. ‡, Doherty, P. C., Grosveld, G., Paul, W. E., and Ihle, J. N. (1996) Lack of IL-4-induced Th2 response in IgE class switching in mice with disrupted Stat6 gene. *Nature 380*, 630–633.

(29) Sha, W. C., Liou, H., Tuomanen, E. I., and Baltimore, D. (1995) Targeted Disruption of the p50 Subunit of NF-KB Leads to Multifocal Defects in Immune Responses. *Cell 80*, 321–330.

(30) Thienes, C. P., Monte, L. D., Monticelli, S., Busslinger, M., Could, H. J., and Vercelli, D. (1997) The Transcription Factor B Cell-Specific Activator Protein (BSAP) Enhances Both IL-4- and CD40-Mediated Activation of the Human. *The Journal of Immunology 22*, 5874–5882.

(31) Stütz, a M., and Woisetschläger, M. (1999) Functional synergism of STAT6 with either NF-kappa B or PU.1 to mediate IL-4-induced activation of IgE germline gene transcription. *Journal of immunology 163*, 4383–4391.

(32) Delphin, B. S., and Stavnezer, J. (1995) Characterization of a interleukin 4 (IL-4) rponsive region in the immunoglobulin heavy chain germline E promoter: Regulation by NF-IL-4, a C/EBP family member and NF-kB/p50. *Journal of experimental medicine 181*, 181–192.

(33) Mao, C. S., and Stavnezer, J. (2001) Differential regulation of mouse germline Ig gamma 1 and epsilon promoters by IL-4 and CD40. *Journal of immunology 167*, 1522–1534.

(34) Sugai, M., Gonda, H., Kusunoki, T., Katakai, T., Yokota, Y., and Shimizu, A. (2003) Essential role of Id2 in negative regulation of IgE class switching. *Nature immunology 4*, 25–30.

(35) Harris, M. B., Chang, C., Berton, M. T., Danial, N., Zhang, J., Kuehner, D., Ye, B. H., Kvatyuk, M., Pandolfi, P. P., Cattoretti, G., Dalla-favera, R., Rothman, P. B., and Danial, N. N. (1999) Transcriptional Repression of Stat6-Dependent Interleukin-4-Induced Genes by BCL-6 : Specific Regulation of Iε Transcription and Immunoglobulin E Switching. *Molecular and cellular biology 19*, 7264–7275.

(36) Yokota, Y., Mansouri, A., and Mori, S. (1999) Development of peripheral lymphoid organs and natural killer cells depends on the helix ± loop ± helix inhibitor Id2. *Nature 397*, 702–706.

(37) Yamada, T., Zhu, D., Saxon, A., and Zhang, K. (2002) CD45 controls interleukin-4-mediated IgE class switch recombination in human B cells through its function as a Janus kinase phosphatase. *The Journal of biological chemistry 277*, 28830–28835.

(38) Zhou, C., Saxon, A., Zhang, K., and Alerts, E. (2013) Human Activation-Induced Cytinide Deaminase Is Induced by IL-4 and Negatively Regulated by CD45: Implication of CD45 as a Janus Kinase Phosphatase in Antibody Diversification. *The Journal of Immunology 170*, 1887–1893.

(39) Elliott, J., and Johnston, J. A. (2004) SOCS: role in inflammation, allergy and homeostasis. *Trends in immunology 25*, 434–440.

(40) Pioli, C., Gatta, L., Ubaldi, V., and Doria, G. (2000) Inhibition of IgG1 and IgE production by stimulation of the B cell CTLA-4 receptor. *Journal of immunology 165*, 5530–5536.

(41) Rush, J. S., Hasbold, J., and Hodgkin, P. D. (2002) Cross-linking surface Ig delays CD40 ligand- and IL-4-induced B cell Ig class switching and reveals evidence for independent regulation of B cell proliferation and differentiation. *Journal of immunology 168*, 2676–2682.

(42) King, C. L., Gallint, J. I., Malecht, H. L., Stuart, L., and Nutman, T. B. (1989) Regulation of immunoglobulin production in hyperimmuno- globulin E recurrent-infection syndrome by interferon y. *PNAS 86*, 10085–10089.

(43) Sherr, E., Macy, E., Kimata, H., Gilly, M., and Saxon, A. (1989) Binding the low affinity Fc epsilon R on B cells suppresses ongoing human IgE synthesis. *Journal of immunology 142*, 481–489.

(44) Yu, P., Kosco-Vilbois, M., Richards, M., Kohler, G., and Lamers, M. C. (1994) Regative feedback regulation of IgE synthesis by murine CD23. *Nature 369*, 753–756.

(45) Danso-Abeam, D., Zhang, J., Dooley, J., Staats, K. a, Van Eyck, L., Van Brussel, T., Zaman, S., Hauben, E., Van de Velde, M., Morren, M.-A., Renard, M., Van Geet, C., Schaballie, H., Lambrechts, D., Tao, J., Franckaert, D., Humblet-Baron, S., Meyts, I., and Liston, A. (2013) Olmsted syndrome: exploration of the immunological phenotype. *Orphanet journal of rare diseases 8*, 79–86.

(46) Felgentreff, K., Perez-Becker, R., Speckmann, C., Schwarz, K., Kalwak, K., Markelj, G., Avcin, T., Qasim, W., Davies, E. G., Niehues, T., and Ehl, S. (2011) Clinical and immunological manifestations of patients with atypical severe combined immunodeficiency. *Clinical immunology 141*, 73–82.

(47) Liston, A., Enders, A., and Siggs, O. M. (2008) Unravelling the association of partial T-cell immunodeficiency and immune dysregulation. *Nature Reviews Immunology 8*, 545–558.

(48) Ozcan, E., Notarangelo, L. D., and Geha, R. S. (2008) Primary immune deficiencies with aberrant IgE production. *The Journal of allergy and clinical immunology 122*, 1054–1062.

(49) Freeman, A. F., and Holland, S. M. (2010) Clinical Manifestations, Etiology, and Pathogenesis of the Hyper IgE Syndromes. *Pediatric Research 65*, 32–37.

(50) Zhang, Q., and Su, H. C. (2011) Hyperimmunoglobulin E syndromes in pediatrics. *Current Opinion in Pediatrics 23*, 653–658.

(51) Szczawinska-Poplonyk, A., Kycler, Z., Pietrucha, B., Heropolitanska-Pliszka, E., Breborowicz, A., and Gerreth, K. (2011) The hyperimmunoglobulin E syndrome--clinical manifestation diversity in primary immune deficiency. *Orphanet journal of rare diseases 6*, 76–86.

(52) Sowerwine, K. J., Holland, S. M., and Freeman, A. F. (2012) Hyper-IgE syndrome update. *Annals of the New York Academy of Sciences 1250*, 25–32.

(53) Grimbacher, B., Holland, S. M., and Puck, J. M. (2005) Hyper-IgE syndromes. *Immunological Reviews 203*, 244–250.

(54) Freeman, A. F., Kleiner, D. E., Nadiminti, H., Davis, J., Quezado, M., Anderson, V., Puck, J. M., and Holland, S. M. (2007) Causes of death in hyper-IgE syndrome. *The Journal of allergy and clinical immunology 119*, 1234–1240.

(55) Randall, K. L., Lambe, T., Johnson, A. L., Johnson, A., Treanor, B., Kucharska, E., Domaschenz, H., Whittle, B., Tze, L. E., Enders, A., Crockford, T. L., Bouriez-Jones, T., Alston, D., Cyster, J. G., Lenardo, M. J., Mackay, F., Deenick, E. K., Tangye, S. G., Chan, T. D., Camidge, T., Brink, R., Vinuesa, C. G., Batista, F. D., Cornall, R. J., and Goodnow, C. C. (2009) Dock8 mutations cripple B cell immunological synapses, germinal centers and long-lived antibody production. *Nature immunology 10*, 1283–1291.

(56) Minegishi, Y. (2009) Hyper-IgE syndrome. *Current opinion in immunology 21*, 487–492.

(57) Hill, H. R., Quie, P. G., Pabst, H. F., Ochs, H. D., Clark, R. A., and Klebanoff, S. J. (1974) Defect in Neutrophil granulocyte chemotaxis in Job's syndrome of abscesses IgE. *The Lancet 2*, 617–619.

(58) Milner, J. D., Brenchley, J. M., Laurence, A., Freeman, A. F., Hill, B. J., Elias, K. M., Kanno, Y., Spalding, C., Elloumi, H. Z., Paulson, M. L., Davis, J., Hsu, A., Asher, A. I., O'Shea, J., Holland, S. M., Paul, W. E., and Douek, D. C. (2008) Impaired T(H)17 cell differentiation in subjects with autosomal dominant hyper-IgE syndrome. *Nature 452*, 773–776.

(59) Dong, C. (2008) TH17 cells in development: an updated view of their molecular identity and genetic programming. *Nature Reviews Immunology 8*, 337–348.

(60) Yang, X. O., Panopoulos, A. D., Nurieva, R., Chang, S. H., Wang, D., Watowich, S. S., and Dong, C. (2007) STAT3 regulates cytokine-mediated generation of inflammatory helper T cells. *The Journal of biological chemistry 282*, 9358–9363.

(61) Gaffen, S. L. (2008) An overview of IL-17 function and signaling. *Cytokine 43*, 402–407.

(62) Saito, M., Nagasawa, M., Takada, H., Hara, T., Tsuchiya, S., Agematsu, K., Yamada, M., Kawamura, N., Ariga, T., Tsuge, I., Nonoyama, S., Karasuyama, H., and Minegishi, Y. (2011) Defective IL-10 signaling in hyper-IgE syndrome results in impaired generation of tolerogenic dendritic cells and induced regulatory T cells. *The Journal of experimental medicine 208*, 235–249.

(63) Minegishi, Y., and Saito, M. (2011) Molecular mechanisms of the immunological abnormalities in hyper-IgE syndrome. *Annals of the New York Academy of Sciences 1246*, 34–40.

(64) Verbsky, J. W., and Chatila, T. a. (2011) T-regulatory cells in primary immune deficiencies. *Current opinion in allergy and clinical immunology 11*, 539–544.

(65) Zhang, Q., Davis, J. C., Lamborn, I. T., Freeman, A. F., Jing, H., Ph, D., Favreau, A. J., Matthews, H. F., Davis, J., Turner, M. L., Uzel, G., Holland, S. M., and Su, H. C. (2009) Combined Immunodeficiency Associated with DOCK8 Mutations. *The New England journal of medicine 361*, 2046–2055.

(66) Lambe, T., Crawford, G., Johnson, A. L., Crockford, T. L., Bouriez-Jones, T., Smyth, A. M., Pham, T. H. M., Zhang, Q., Freeman, A. F., Cyster, J. G., Su, H. C., and Cornall, R. J. (2011) DOCK8 is essential for T-cell survival and the maintenance of CD8+ T-cell memory. *European journal of immunology 41*, 3423–3435.

(67) Randall, K. L., Chan, S. S.-Y., Ma, C. S., Fung, I., Mei, Y., Yabas, M., Tan, A., Arkwright, P. D., Al Suwairi, W., Lugo Reyes, S. O., Yamazaki-Nakashimada, M. a, Garcia-Cruz, M. D. L. L., Smart, J. M., Picard, C., Okada, S., Jouanguy, E., Casanova, J.-L., Lambe, T., Cornall, R. J., Russell, S., Oliaro, J., Tangye, S. G., Bertram, E. M., and Goodnow, C. C. (2011) DOCK8 deficiency impairs CD8 T cell survival and function in humans and mice. *The Journal of experimental medicine 208*, 2305–2320.

(68) Mizesko, M. C., Banerjee, P. P., Monaco-Shawver, L., Mace, E. M., Bernal, W. E., Sawalle-Belohradsky, J., Belohradsky, B. H., Heinz, V., Freeman, A. F., Sullivan, K. E., Holland, S. M., Torgerson, T. R., Al-Herz, W., Chou, J., Hanson, I. C., Albert, M. H., Geha, R. S., Renner, E. D., and Orange, J. S. (2013) Defective actin accumulation impairs human natural killer cell function in patients with dedicator of cytokinesis 8 deficiency. *The Journal of allergy and clinical immunology 131*, 840–848.

(69) Engelhardt, K. R., McGhee, S., Winkler, S., Sassi, A., Woellner, C., Lopez-Herrera, G., Chen, A., Kim, H. S., Lloret, M. G., Schulze, I., Ehl, S., Thiel, J., Pfeifer, D., Veelken, H., Niehues, T., Siepermann, K., Weinspach, S., Reisli, I., Keles, S., Genel, F., Kutukculer, N., Kutuculer, N., Camcioğlu, Y., Somer, A., Karakoc-Aydiner, E., Barlan, I., Gennery, A., Metin, A., Degerliyurt, A., Pietrogrande, M. C., Yeganeh, M., Baz, Z., Al-Tamemi, S., Klein, C., Puck, J. M., Holland, S. M., McCabe, E. R. B., Grimbacher, B., and Chatila, T. a. (2009) Large deletions and point mutations involving the dedicator of cytokinesis 8 (DOCK8) in the autosomal-recessive form of hyper-IgE syndrome. *The Journal of allergy and clinical immunology 124*, 1289–1302.

(70) Chu, E. Y., Freeman, A. F., Jing, H., Cowen, E. W., Davis, J., Su, H. C., Holland, S. M., and Turner, M. L. C. (2012) Cutaneous manifestations of DOCK8 deficiency syndrome. *Archives of dermatology 148*, 79–84.

(71) Su, H. C., Jing, H., and Zhang, Q. (2011) DOCK8 deficiency. *Annals of the New York Academy of Sciences 1246*, 26–33.

(72) Minegishi, Y., Saito, M., Morio, T., Watanabe, K., Agematsu, K., Tsuchiya, S., Takada, H., Hara, T., Kawamura, N., Ariga, T., Kaneko, H., Kondo, N., Tsuge, I., Yachie, A., Sakiyama, Y., Iwata, T., Bessho, F., Ohishi, T., Joh, K., Imai, K., Kogawa, K., Shinohara, M., Fujieda, M., Wakiguchi, H., Pasic, S., Abinun, M., Ochs, H. D., Renner, E. D., Jansson, A., Belohradsky, B. H., Metin, A., Shimizu, N., Mizutani, S., Miyawaki, T., Nonoyama, S., and Karasuyama, H. (2006) Human tyrosine kinase 2 deficiency reveals its requisite roles in multiple cytokine signals involved in innate and acquired immunity. *Immunity 25*, 745–755.

(73) Shaw, M. H., Freeman, G. J., Scott, M. F., Fox, B. a, Bzik, D. J., Belkaid, Y., and Yap, G. S. (2006) Tyk2 negatively regulates adaptive Th1 immunity by mediating IL-10 signaling and promoting IFN-gamma-dependent IL-10 reactivation. *Journal of immunology 176*, 7263–7271.

(74) Shimoda, K., Kato, K., Aoki, K., Matsuda, T., Miyamoto, A., Shibamori, M., Yamashita, M., Numata, A., Takase, K., Kobayashi, S., Shibata, S., Asano, Y., Gondo, H., Sekiguchi, K., Nakayama, K., Nakayama, T., Okamura, T., Okamura, S., and Niho, Y. (2000) Tyk2 plays a restricted role in IFN alpha signaling, although it is required for IL-12-mediated T cell function. *Immunity 13*, 561–571.

(75) Minegishi, Y., and Saito, M. (2012) Cutaneous manifestations of Hyper IgE syndrome. *Allergology international 61*, 191–196.

(76) Grimbacher, B., Schäffer, A. A., Holland, S. M., Davis, J., Gallin, J., and Malech, H. (1999) Genetic linkage of hyper-IgE syndrome to chromosome 4. *American journal of human genetics 65*, 735–744.

(77) Oyoshi, M. K., Mufphy, G. F., and Geha, R. S. (2010) Filaggrin deficient mice exhibit Th17-dominated skin inflammation and permissiveness to epicutaneous sensitization with protein antigen. *Journal of allergy and clinical immunology 124*, 485–493.

(78) Kawasaki, H., Nagao, K., Kubo, A., Hata, T., Shimizu, A., Mizuno, H., Yamada, T., and Amagai, M. (2012) Altered stratum corneum barrier and enhanced percutaneous immune responses in filaggrin-null mice. *The Journal of allergy and clinical immunology 129*, 1538–1546.

(79) Weidinger, S., Gieger, C., Rodriguez, E., Baurecht, H., Mempel, M., Klopp, N., Gohlke, H., Wagenpfeil, S., Ollert, M., Ring, J., Behrendt, H., Heinrich, J., Novak, N., Bieber, T., Krämer, U., Berdel, D., Von Berg, A., Bauer, C. P., Herbarth, O., Koletzko, S., Prokisch, H., Mehta, D., Meitinger, T., Depner, M., Von Mutius, E., Liang, L., Moffatt, M., Cookson, W., Kabesch, M., Wichmann, H.-E., and Illig, T. (2008) Genome-wide scan on total serum IgE levels identifies FCER1A as novel susceptibility locus. *PLoS genetics 4*, 1–9.

(80) Moffatt, M. F., Gut, I. G., Demenais, F., Strachan, D. P., Bouzigon, E., Heath, S., Von Mutius, E., Farrall, M., Lathrop, M., and Cookson, W. O. C. M. (2010) A large-scale, consortium-based genomewide association study of asthma. *The New England journal of medicine 363*, 1211–1221.

(81) Jun, J. E., Wilson, L. E., Vinuesa, C. G., Lesage, S., Blery, M., Miosge, L. a, Cook, M. C., Kucharska, E. M., Hara, H., Penninger, J. M., Domashenz, H., Hong, N. a, Glynne, R. J., Nelms, K. a, and Goodnow, C. C. (2003) Identifying the MAGUK protein Carma-1 as a central regulator of humoral immune responses and atopy by genome-wide mouse mutagenesis. *Immunity 18*, 751–762.

(82) Blonska, M., Joo, D., Zweidler-McKay, P. a, Zhao, Q., and Lin, X. (2012) CARMA1 controls Th2 cell-specific cytokine expression through regulating JunB and GATA3 transcription factors. *Journal of immunology 188*, 3160–3168.

(83) Altin, J. a, Tian, L., Liston, A., Bertram, E. M., Goodnow, C. C., and Cook, M. C. (2011) Decreased T-cell receptor signaling through CARD11 differentially compromises forkhead box protein 3-positive regulatory versus T(H)2 effector cells to cause allergy. *The Journal of allergy and clinical immunology 127*, 1277–1285.

(84) Chiang, Y. J., Sommers, C. L., Jordan, M. S., Gu, H., Samelson, L. E., Koretzky, G. a, and Hodes, R. J. (2004) Inactivation of c-Cbl reverses neonatal lethality and T cell developmental arrest of SLP-76-deficient mice. *The Journal of experimental medicine 200*, 25–34.

(85) Huppler, A. R., Bishu, S., and Gaffen, S. L. (2012) Mucocutaneous candidiasis : the IL-17 pathway and implications for targeted immunotherapy. *Arthritis research and therapy 14*, 217–225.

(86) Ford, J. W., Sturgill, J. L., and Conrad, D. H. (2009) 129/SvJ mice have mutated CD23 and hyper IgE. *Cellular immunology 254*, 124–134.

(87) Bottema, R. W. B., Postma, D. S., Reijmerink, N. E., Thijs, C., Stelma, F. F., Smit, H. a, Van Schayck, C. P., Brunekreef, B., Koppelman, G. H., and Kerkhof, M. (2010) Interaction of T-cell and antigen presenting cell co-stimulatory genes in childhood IgE. *The European respiratory journal 35*, 54–63.

(88) Takahashi, S., Futatsugi-Yumikura, S., Fukuoka, A., Yoshimoto, T., Nakanishi, K., and Yonehara, S. (2012) Fas deficiency in mice with the Balb/c background induces blepharitis with allergic inflammation and hyper-IgE production in conjunction with severe autoimmune disease. *International immunology 109*, 1–7.

(89) Matsumoto, R., Wang, D., Blonska, M., Li, H., Kobayashi, M., Pappu, B., Chen, Y., Wang, D., and Lin, X. (2005) Phosphorylation of CARMA1 plays a critical role in T Cell receptor-mediated NF-kappaB activation. *Immunity 23*, 575–585.

(90) Hara, H., Wada, T., Bakal, C., Kozieradzki, I., Suzuki, S., Suzuki, N., Nghiem, M., Griffiths, E. K., Krawczyk, C., Bauer, B., D'Acquisto, F., Ghosh, S., Yeh, W. C., Baier, G., Rottapel, R., and Penninger, J. M. (2003) The MAGUK family protein CARD11 is essential for lymphocyte activation. *Immunity 18*, 763–775.

(91) Molinero, L. L., Cubre, A., Mora-Solano, C., Wang, Y., and Alegre, M.-L. (2012) T cell receptor/CARMA1/NF-κB signaling controls T-helper (Th) 17 differentiation. *Proceedings of the National Academy of Sciences of the United States of America 109*, 18529–18534.

(92) Stepensky, P., Keller, B., Buchta, M., Kienzler, A.-K., Elpeleg, O., Somech, R., Cohen, S., Shachar, I., Miosge, L. a, Schlesier, M., Fuchs, I., Enders, A., Eibel, H., Grimbacher, B., and Warnatz, K. (2013) Deficiency of caspase recruitment domain family, member 11 (CARD11), causes profound combined immunodeficiency in human subjects. *The Journal of allergy and clinical immunology 131*, 477–485.

(93) Greil, J., Rausch, T., Giese, T., Bandapalli, O. R., Daniel, V., Bekeredjian-Ding, I., Stütz, A. M., Drees, C., Roth, S., Ruland, J., Korbel, J. O., and Kulozik, A. E. (2013) Whole-exome sequencing links caspase recruitment domain 11 (CARD11) inactivation to severe combined immunodeficiency. *The Journal of allergy and clinical immunology 131*, 1376–1383.

(94) Medoff, B. D., Seed, B., Jackobek, R., Yang, Y., Luster, A. D., Xavier, R., and Zora, J. (2006) Allergic Airway Inflammation in a Murine CARMA1 Is Critical for the Development of Model of Asthma. *The Journal of Immunology 176*, 7272–7277.

(95) Wang, J.-L., Cao, L., Li, X.-H., Hu, Z.-M., Li, J.-D., Zhang, J.-G., Liang, Y., San-A, Li, N., Chen, S.-Q., Guo, J.-F., Jiang, H., Shen, L., Zheng, L., Mao, X., Yan, W.-Q., Zhou, Y., Shi, Y.-T., Ai, S.-X., Dai, M.-Z., Zhang, P., Xia, K., Chen, S.-D., and Tang, B.-S. (2011) Identification of PRRT2 as the causative gene of paroxysmal kinesigenic dyskinesias. *Brain 134*, 3493–3501.

(96) Li, R., Yu, C., Li, Y., Lam, T., Yiu, S., Kristiansen, K., and Wang, J. (2009) SOAP2: an improved ultrafast tool for short read alignment. *Bioinformatics 25*, 1966–1967.

(97) Li, R., Li, Y., Fang, X., Yang, H., Wang, J., and Kristiansen, K. (2009) SNP detection for massively parallel whole-genome resequencing. *Genome Res 19*, 1124–1132.

(98) McKenna, A., Hanna, M., Banks, E., Sivachenko, A., Cibulskis, K., Kernytsky, A., Garimella, K., Altshuler, D., Gabriel, S., Daly, M., and DePristo, M. (2010) The Genome Analysis Toolkit: a MapReduce framework for analyzing next-generation DNA sequencing data. *Genome Res 20*, 1297–1303.

(99) Li, H., and Durbin, R. (2010) Fast and accurate long-read alignment with Burrows-Wheeler transform. *Bioinformatics 26*, 589–595.

(100) Jurinke, C., Oeth, P., and Van den Boom, D. (2004) MALDI-TOF mass spectrometry: a versatile tool for high-performance DNA analysis. *Mol Biotechnol 26*, 147–164.

(101) Andreas Untergasser, Nijveen, H., Rao, X., Bisseling, T., Geurts, R., and Leunissen, J. A. M. (2007) Primer3Plus, an enhanced web interface to Primer3. *Nucleic Acids Research 35*, 71–74.

(102) Adzhubei, I. a, Schmidt, S., Peshkin, L., Ramensky, V. E., Gerasimova, A., Bork, P., Kondrashov, A. S., and Sunyaev, S. R. (2010) A method and server for predicting damaging missense mutations. *Nature methods 7*, 248–249.

(103) Sim, N.-L., Kumar, P., Hu, J., Henikoff, S., Schneider, G., and Ng, P. C. (2012) SIFT web server: predicting effects of amino acid substitutions on proteins. *Nucleic acids research 40*, 452–457.

(104) Jeelall, Y. S., Wang, J. Q., Law, H.-D., Domaschenz, H., Fung, H. K. H., Kallies, A., Nutt, S. L., Goodnow, C. C., and Horikawa, K. (2012) Human lymphoma mutations reveal CARD11 as the switch between self-antigen-induced B cell death or proliferation and autoantibody production. *The Journal of experimental medicine 209*, 1907–1917.

(105) Krampera, M., Antico, A., Vinante, F., Morosato, L., and Pizzolo, G. (1999) Lymphocyte membrane antigen expression and intracellular cytokine patterns in an asymptomatic patient with persistently high serum levels of IgE. *Annals of allergy, asthma & immunology 83*, 144–148.

(106) Ives, M. L., Ma, C. S., Palendira, U., Chan, A., Bustamante, J., Boisson-Dupuis, S., Arkwright, P. D., Engelhard, D., Averbuch, D., Magdorf, K., Roesler, J., Peake, J., Wong, M., Adelstein, S., Choo, S., Smart, J. M., French, M. a, Fulcher, D. a, Cook, M. C., Picard, C., Durandy, A., Tsumura, M., Kobayashi, M., Uzel, G., Casanova, J.-L., Tangye, S. G., and Deenick, E. K. (2013) Signal transducer and activator of transcription 3 (STAT3) mutations underlying autosomal dominant hyper-IgE syndrome impair human CD8(+) T-cell memory formation and function. *The Journal of allergy and clinical immunology 132*, 400–411.

(107) Mazerolles, F., Picard, C., Kracker, S., Fischer, A., and Durandy, A. (2013) Blood CD4+CD45RO+CXCR5+ T cells are decreased but partially functional in signal transducer and activator of transcription 3 deficiency. *Journal of Allergy and Clinical Immunology 131*, 1146–1156.

(108) Snow, A. L., Xiao, W., Stinson, J. R., Lu, W., Chaigne-Delalande, B., Zheng, L., Pittaluga, S., Matthews, H. F., Schmitz, R., Jhavar, S., Kuchen, S., Kardava, L., Wang, W., Lamborn, I. T., Jing, H., Raffeld, M., Moir, S., Fleisher, T. a, Staudt, L. M., Su, H. C., and Lenardo, M. J. (2012) Congenital B cell lymphocytosis explained by novel germline CARD11 mutations. *The Journal of experimental medicine 209*, 2247–2261.

(109) Lenz, G., Davis, R. E., Ngo, V. N., Lam, L., George, T. C., Wright, G. W., Dave, S. S., Zhao, H., Xu, W., Rosenwald, A., Ott, G., Muller-Hermelink, H. K., Gascoyne, R. D., Connors, J. M., Rimsza, L. M., Campo, E., Jaffe, E. S., Delabie, J., Smeland, E. B., Fisher, R. I., Chan, W. C., and Staudt, L. M.

(2008) Oncogenic CARD11 mutations in human diffuse large B cell lymphoma. *Science 319*, 1676–1679.

(110) Ngo, V. N., Davis, R. E., Lamy, L., Yu, X., Zhao, H., Lenz, G., Lam, L. T., Dave, S., Yang, L., Powell, J., and Staudt, L. M. (2006) A loss-of-function RNA interference screen for molecular targets in cancer. *Nature 441*, 106–110.